

ACID-FUNCTIONALIZED NANOPARTICLES FOR HYDROLYSIS OF  
LIGNOCELLULOSIC FEEDSTOCKS

by

LEIDY E. PEÑA DUQUE

B.Sc., National University of Colombia, Medellin, Colombia, 2004

A THESIS

submitted in partial fulfillment of the requirements for the degree

MASTER OF SCIENCE

Department of Biological and Agricultural Engineering  
College of Engineering

KANSAS STATE UNIVERSITY  
Manhattan, Kansas

2009

Approved by:

Major Professor  
Dr. Donghai Wang

## Abstract

Acid catalysts have been successfully used for pretreatment of cellulosic biomass to improve sugar recovery and its later conversion to ethanol. However, use of acid requires a considerable equipment investment as well as disposal of residues. Acid-functionalized nanoparticles were synthesized for pretreatment and hydrolysis of lignocellulosic biomass to increase conversion efficiency at mild conditions. Advantages of using acid-functionalized metal nanoparticles are not only the acidic properties to catalyze hydrolysis and being small enough to penetrate into the lignocellulosic structure, but also being easily separable from hydrolysis residues by using a strong magnetic field.

Cobalt spinel ferrite magnetic nanoparticles were synthesized using a microemulsion method and then covered with a layer of silica to protect them from oxidation. The silanol groups of the silica serve as the support of the sulfonic acid groups that were later attached to the surface of the nanoparticles. TEM images and FTIR methods were used to characterize the properties of acid-functionalized nanoparticles in terms of nanoparticle size, presence of sulfonic acid functional groups, and pH as an indicator of acid sites present. Citric acid-functionalized magnetite nanoparticles were also synthesized and evaluated.

Wheat straw and wood fiber samples were treated with the acid supported nanoparticles at 80°C for 24 h to hydrolyze their hemicellulose fraction to sugars. Further hydrolysis of the liquid fraction was carried out to account for the amount of total solubilized sugars. HPLC was used to determine the total amount of sugars obtained in the aqueous solution. The perfluoroalkyl-sulfonic acid functional groups from the magnetic nanoparticles yielded significantly higher amounts of oligosaccharides from wood and wheat straw samples than the alkyl-sulfonic acid functional groups did. More

stable fluorosulfonic acid functionalized nanoparticles can potentially work as an effective heterogeneous catalyst for pretreatment of lignocellulosic materials.

# Table of Contents

List of Figures.....	vi
List of Tables.....	viii
Acknowledgements .....	ix
CHAPTER 1 - Introduction .....	1
General Background.....	1
CHAPTER 2 - Literature Review .....	4
2.1 Biomass Structure and Composition.....	4
2.2 Biomass Pretreatment Methods .....	5
2.2.1 Acid Hydrolysis.....	6
2.2.2 Alkaline Hydrolysis .....	6
2.2.3 Hot Compressed Water.....	7
2.2.4 Steam Explosion .....	7
2.2.5 Ammonia Fiber Explosion .....	8
2.2.6 Supercritical CO <sub>2</sub> Pretreatment .....	9
2.3 Enzymatic Hydrolysis.....	9
2.4 Nanocatalyst to Mimic Enzymes.....	10
2.4.1 Acid-Supported Materials .....	11
2.4.2 Acid Functionalization of Silica.....	11
2.4.3 Silica-Supported Perfluoroalkyl-sulfonic Acids .....	12
2.4.4 Acid Strength of Sulfonic Supported Acids.....	14
2.5 Solid Supported Acids for Cellulose Hydrolysis .....	15
CHAPTER 3 - Synthesis and Characterization of Acid-functionalized Magnetic Nanoparticles.....	18
3.1 Introduction.....	18
3.2 Materials and Methods .....	20
3.2.1 Chemicals .....	20
3.2.2 Sonication .....	20
3.2.3 TEM Images.....	21
3.2.4 FTIR Analysis.....	21

3.2.5 Preparation of Magnetic Nanoparticles (MNPs) .....	21
3.2.6 Silica Coating of the Magnetic Nanoparticles (SiMNPs).....	22
3.2.7 Acid Functionalization of the Silica-coated Magnetic Nanoparticles.....	22
3.4 Results and Discussion .....	24
3.4.1 Particles Size and Distribution of Synthesized Nanoparticles .....	24
3.4.2 FTIR Spectrum.....	31
3.4.3 Acid Loading .....	33
3.5 Conclusions .....	34
CHAPTER 4 - Biomass Pretreatment Using Acid-Functionalized Magnetic Nanoparticles	
.....	36
4.1 Introduction.....	36
4.2 Materials and Methods .....	38
4.2.1 Hydrolysis of Biomass .....	38
4.2.2 Total Carbohydrates Analysis: .....	39
4.2.3 Enzymatic Hydrolysis .....	39
4.3 Results and Discussion .....	40
4.3.1 Monosaccharides Yield .....	40
4.3.2 Total Sugars Yield.....	42
4.3.4 Hydrolysis of extractives-free Wood Fiber and Wheat Straw .....	44
4.3.5 Enzymatic Hydrolysis .....	46
4.3.6 Effect of the pH .....	47
4.3.7 Performance of the Catalysts .....	49
4.3.8 Effect of Temperature.....	50
4.4 Conclusions .....	51
CHAPTER 5 - Conclusions and Recommendations for Further Research.....	53
5.2 Recommendations.....	54

## List of Figures

Figure 2-1 Structure of different biomass fractions (modified from Iborra et al. 2006).....	5
Figure 2-2 Acid-functionalized silicas representation .....	12
Figure 2-3 Flurosulfonic acid resin Nafion® SAC-13.....	14
Figure 2-4 Cellulose Conversion using amorphous carbon with sulfonic groups (Adopted from Suganuma et al. 2008).....	17
Figure 3-1 Schematic representation for AS-SiMNPs preparation (Adopted from Gill et al. 2007) .....	23
Figure 3-2 Schematic representation for HPS-SiMNPs preparation (Adopted from Gill et al. 2007) .....	24
Figure 3-3 Cobalt spinel ferrite nanoparticles (100 nm scale) .....	25
Figure 3-4 Cobalt spinel ferrite nanoparticles (20nm scale) .....	25
Figure 3-5 Silica-coated cobalt spinel ferrite nanoparticles (500 nm scale).....	26
Figure 3-6 Silica-coated cobalt spinel ferrite nanoparticles (100 nm scale).....	26
Figure 3-7 Silica-coated cobalt spinel ferrite nanoparticles (left, 100 nm scale; right, 20 nm scale).....	27
Figure 3-8 Histogram for silica-coated nanoparticles .....	28
Figure 3-9 Perfluoroalkyl-sulfonic acid nanoparticles (left, 100 nm scale; right 20 nm scale) .....	29
Figure 3-10 Alkyl-sulfonic-acid nanoparticles (100 nm scale) .....	30
Figure 3-11 Histogram for the AS-SiMNPs.....	30
Figure 3-12 FTIR spectra of silica-coated nanoparticles .....	31
Figure 3-13 FTIR spectra of alkyl-sulfonic acid nanoparticles .....	32
Figure 3-14 FTIR spectra of perfluoroalkyl-sulfonic-acid nanoparticles.....	33
Figure 4-1 Monomer sugars and cellobiose yields from wheat straw after pretreated with PFS and AS acid functionalized nanoparticles at 80°C for 24h.....	41
Figure 4-2 Monomer sugars and cellobiose yields from wood fiber after pretreated with PFS acid functionalized nanoparticles at 80°C for 2 4h .....	41

Figure 4-3 Total sugar yield from wheat straw after pretreated with PFS and AS acid functionalized nanoparticles at 80°C for 24h..... 42

Figure 4-4 Total sugar yield from wood fiber after pretreated with PFS acid functionalized nanoparticles at 80°C for 24h..... 43

Figure 4-5 Monomer sugars yield and cellobiose from wheat straw extractives free after pretreated with PFS acid functionalized nanoparticles at 80°C for 24h..... 44

Figure 4-6 Total sugar yield from wheat straw extractives free after pretreated with PFS acid functionalized nanoparticles at 80°C for 24h .. 45

Figure 4-7 Monomer sugars yield and cellobiose from wood fiber extractives free after pretreated with PFS acid functionalized nanoparticles at 80°C for 24h..... 45

Figure 4-8 Total sugar yield from wood fiber extractives free after pretreated with PFS acid functionalized nanoparticles at 80°C for 24h .. 46

Figure 4-9 pH vs sugar yield plot for wheat straw and wood fiber, extractives free..... 49

## List of Tables

Table 2-1 Acid loading of some solid acids .....	15
Table 2-2 Glucose yields from oligosaccharides using solid acid catalyst.....	16
Table 3-1 Acid Capacity Titration .....	34
Table 4-1 Biomass compositional analysis.....	39
Table 4-2 Digestibility of biomass after pretreatment with acid catalysts .....	47
Table 4-3 pH of the solution at the end of pretreatment .....	48
Table 4-4 Sulfonic acid loading before and after reaction .....	50
Table 4-5 Hemicellulose yield from wood fiber hydrolysis at 120°C for 2h.....	51

## **Acknowledgements**

Thanks to Dr. Donghai Wang for his support and guidance for carrying out this research toward the completion of my master's program. I also want to thank Dr. Keith Hohn for his help and valuable input in the execution of this project.

I would like to thank Dr. Susan Sun for agreeing to be a member of my committee. I would like to thank William Bartel for providing the citric-acid nanoparticles, Chien Chang and Myles Ikenberry for running the samples to get the FTIR spectra, and Nicholas Chisholm for running the software to get particle size distributions. I want to thank the members of Dr. Wang's research group for their help and cooperation: May, Feng, DeeAnn and Dr. Wu.

Thanks to the faculty and staff in the Department of Biological and Agricultural Engineering at Kansas State University.

# **CHAPTER 1 - Introduction**

## **General Background**

In the U.S. and worldwide, economies have been depending on fossil fuels (coal, oil, and natural gas), which are finite, nonrenewable energy sources. With finite reserves, non-uniform distribution, and volatile prices of fossil fuels, as well as the desire to decrease U.S. dependence on foreign oil, renewable fuels are increasingly being considered as replacements for petroleum-based fuels. The U.S. government recently called for this nation to annually produce 36 billion gallons of renewable fuels by 2022 (Allred et al. 2008). In 2008, about 9.4 billion gallons of fuel ethanol were produced in the U.S. (International Trade Commission and Jim Jordan and Associates 2009). At present, ethanol is produced primarily from corn (97%); however, using 100% of the 2008 corn crop for ethanol production would produce about 36 billion gallons of ethanol; this amount would meet only about 17% of the nation's needs. Furthermore, a dramatic increase in ethanol production using current grain-starch-based technology may be limited by the fact that grain production for ethanol will compete for limited agricultural land also needed for food and feed production. Cellulosic biofuels do not have the same limitations of grain-starch-based biofuel production.

Conversion of cellulosic biomass such as agricultural residues to biofuels offers major economic, environmental, and strategic benefits. DOE and USDA projected that U.S. biomass resources could provide approximately 1.3 billion dry tons of feedstock (998 million dry tons from agricultural residues) for biofuels, which would meet about 40% of the annual U.S. fuel demand for transportation (Perlack et al. 2005). However, production of biofuels from cellulosic biomass faces significant technical challenges. Success depends largely upon the physical and chemical properties of the biomass, pretreatment methods, effective enzyme systems, efficient fermentation microorganisms, and optimization of processing conditions. Pretreatment, enzymatic hydrolysis and fermentation are the three major steps for ethanol production from lignocellulosic biomass. The challenge of producing ethanol from cellulose is the difficulty in breaking down cellulosic matter to sugars. Cellulosic materials are a complex mixture of cellulose, hemicellulose, and lignin. In their original form, the

cellulose of these materials is not readily available for hydrolysis, so pretreatment (both physical and chemical) is usually required. Pretreatment of lignocellulosic biomass is crucial before proceeding to hydrolysis. The purpose of pretreatment is to break the lignin seal, disrupt the crystalline structure of cellulose, and increase the surface area of the cellulose, making the polysaccharides more susceptible to enzyme hydrolysis. The polymers of glucose are joined by glycosidic bonds. These polymers can be hydrolyzed with acid or base solutions or with steam or hot water (Jacobsen and Wyman 2002; Teymouri et al. 2004a; Herrera et al. 2004; Liu 2005). High sugar yields have been reached with acid hydrolysis treatments using sulfuric acid (Corredor et al. 2008). However, even low concentrations of sulfuric acid can cause degradation of glucose to hydroxymethylfurfural and other undesirable compounds (Mosier et al. 2002). Use of sulfuric acid also requires a greater investment because equipment will wear out faster, and waste materials generated from the hydrolysis have to be separated and disposed of. Pretreatment and enzymatic hydrolysis steps account for more than 30% of the cost of cellulosic ethanol (Allred et al. 2008). A variety of degradation products derived from pretreatment of cellulosic biomass could inhibit the normal growth and ethanol fermentation using *Saccharomyces cerevisiae* (Nilsson et al. 2005; Oliva et al. 2006). Detoxification, neutralization, and separation steps have to be applied before enzymatic hydrolysis.

Two primary methods are used for cellulose hydrolysis: mineral acids and enzymes. Mineral acids (most commonly sulfuric acid) have several advantages. They can be used for chemical pretreatment, and they also give fast hydrolysis rates. However, because of the corrosive nature of mineral acids, capital costs are increased due to the need for more expensive construction materials. In addition, costly separation steps are typically required in order to reuse the acid. Enzymes have a number of advantages over mineral acids. First, capital costs should be less because there is no need to buy corrosion-resistant materials. Second, enzymes are much more selective to glucose than mineral acids, which can catalyze decomposition of cellulose. However, enzymes are expensive and cannot be reused, adding to the operating cost of a cellulosic ethanol plant. They are also not capable of catalyzing hydrolysis without pretreatment.

Acid-supported materials have been successfully used for a diverse number of catalytic organic reactions (Alvaro 2005; Bootsma and Shanks 2007; Lien and Zhang 2007). Nanoporous solids with acid sites have shown high catalytic activity in gas and liquid phase reactions (Harmer et al. 2007). Efficient catalysis of the hydrolysis of cellulose was observed using amorphous carbon-bearing acid groups (Suganuma et al. 2008). High cellobiose conversion was obtained using acid organic functionalized mesoporous silica (Bootsma and Shanks 2007). Significant yields of glucose were reported for selective hydrolysis of cellulose using acid zeolites and acid-activated carbon (Onda et al. 2008). Catalytic performance of sulfonic acid-modified mesoporous silica was also evaluated over the hydrolysis of sugars (Dhepe et al. 2005). Because of their tunable properties, functionalized nanoparticles have become an important research subject (Corma and Garcia 2006). Catalytic activity of surface functionalized nanoparticles has recently been studied to mimic biologic reactions (Vriezema et al. 2005). Monodisperse nanoparticles have the advantage of behaving like a fluid solution. The dispersed nanoparticles can't be seen by the naked eye. If the nanoparticles happen to have magnetic behavior, the particles can be recovered by applying a magnetic field (Yoon et al. 2003). Acid-functionalized nanoparticles may have potential as catalysts for pretreatment and hydrolysis of lignocellulosic biomass. Using acid-magnetic functionalized nanoparticles would potentially provide the benefits of acid solutions with the advantage that they can be recovered and reused.

The goal of this research is to develop acid-functionalized nanoparticles for hydrolysis of lignocellulosic feedstocks for biofuel production. Specific objectives of this research are as follows:

1. Synthesis of cobalt spinel ferrite magnetic nanoparticles functionalized with acid functions using alkyl-sulfonic and perfluoroalkyl-sulfonic acid.
2. Characterization of acid-functionalized nanoparticles in terms of particle size, acid functional groups, and pH.
3. Evaluation of the hydrolysis performance of acid-functionalized nanoparticles for sugar production from wheat straw and wood fiber.

## CHAPTER 2 - Literature Review

### 2.1 Biomass Structure and Composition

Agricultural and forest residues, herbage plants, short rotation crops such as willows and poplars, and lignocellulosic crops such as reed canary grass, miscanthus, and switch grass are all considered as renewable biomass. The structure of lignocellulosic biomass is highly complex, and native biomass is resistant to enzymatic hydrolysis. Major composition of biomass feedstocks includes cellulose, hemicellulose, and lignin (Figures 2-1). Cellulose is a polymer of D-glucopyranose monomers linked by  $\beta$ -1,4 bonds. Cellulose is highly crystalline, water insoluble, and highly resistant to depolymerization. Conversely, glucose molecules in starch are linked by  $\alpha$ -1,4 bonds, which are less stable than the aforementioned. The top and bottom moieties of the polymer chain are hydrophobic; in the meantime, the polar hydroxyl groups in the sides give the chain a hydrophilic characteristic (Iborra et al. 2006). The cellulose polymer is embedded in a heteropolymer chain of five and six carbon sugars, hemicellulose. Both of these polymers are protected by lignin layers.

Hemicellulose is a heterogeneous polymer of pentoses (e.g., xylose and arabinose), hexoses (e.g., mannose, glucose or galactose), and sugar acids. Unlike cellulose, hemicelluloses are not chemically homogeneous. Because of its amorphous structure, the hemicellulose polymer is easily hydrolyzed to its monomers. However, the mixture of sugars obtained after hydrolysis makes the conversion to other valuable products such as ethanol, xylitol, and 2,3-butanediol more difficult (Saha 2003). Traditional yeast strains used to ferment sugar to ethanol can not ferment xylose or arabinose to ethanol, and the microorganisms that convert xylose to xylitol can't do it as efficiently in the presence of glucose.

Lignin, on the other hand, is a highly branched polyphenolic resin. The three major phenylpropane units of lignin are p-coumaryl, coniferyl, and sinapyl alcohol. Lignin restricts hydrolysis by shielding cellulose surfaces or by absorbing and inactivating enzymes. It is understood that the close union between lignin and cellulose prevents swelling of the fiber, thereby affecting enzyme accessibility to the cellulose.

The removal of these polymers enhances the enzymatic digestibility of cellulose (Yang and Wyman 2004). As by-products from cellulosic ethanol production, lignin derivatives would be a renewable alternative replacement for current oil-based products such as phenol formaldehyde resins and wood adhesives (Salvado and El Mansouri 2006; Effendi et al. 2008).

Biomass also contains minor compounds classified as extractives and ashes. Water or alcohol extractives can be fats, proteins, starches, monomeric sugars, gums, resins, essential oils, etc. Ash is an inorganic material that the plant could have taken from the soil for its growth.

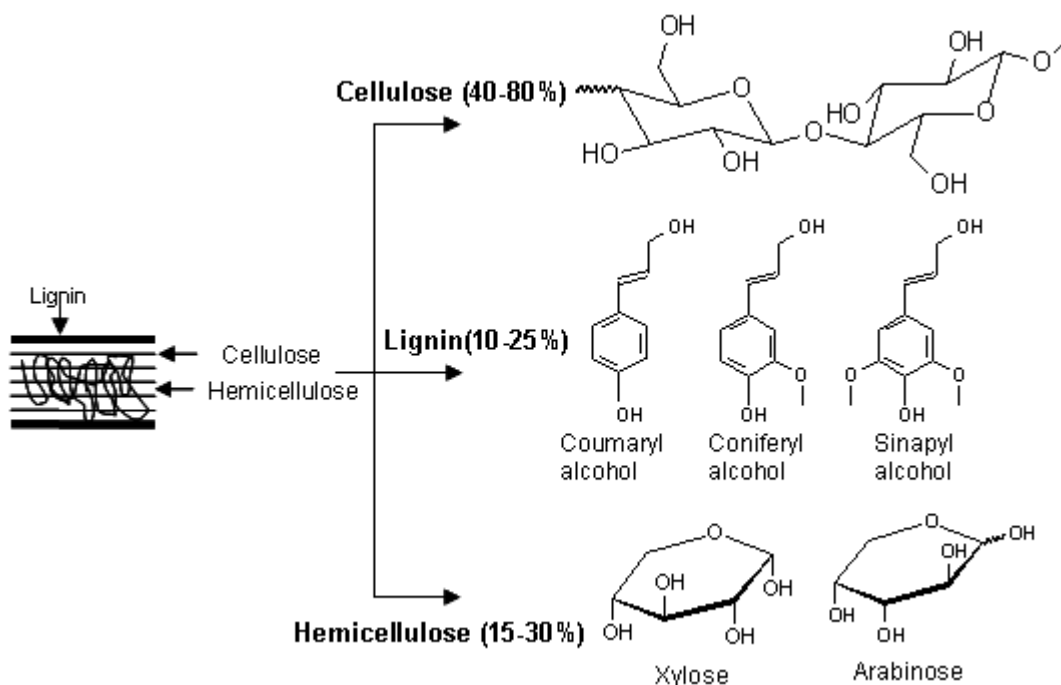


**Figure 2-1 Structure of different biomass fractions (modified from Iborra et al. 2006)**

## 2.2 Biomass Pretreatment Methods

The challenge in producing ethanol from cellulose is the difficulty in breaking down cellulosic matter to monomeric sugars (Iborra et al. 2006). Since the cellulose is not readily available for hydrolysis, pretreatment (both physical and chemical) is usually required. Pretreatment, enzymatic hydrolysis and fermentation are the three major steps for ethanol production from lignocellulosic biomass. The purpose of the

pretreatment method is to break the lignin seal, disrupt the crystalline structure of the cellulose and increase the surface area of the cellulose, making the polysaccharides more susceptible to enzyme hydrolysis. The process is often conducted using mineral acids or basic solutions with steam or hot water (Jacobsen and Wyman 2002; Teymouri et al. 2004a; Herrera et al. 2004; Liu 2005). Dilute-acid treatment, steam explosion, alkaline treatment, ammonia fiber explosion, and supercritical CO<sub>2</sub> and SO<sub>2</sub> are the methods most often used.

### ***2.2.1 Acid Hydrolysis***

Sulfuric acid with concentrations between 0.5% and 2% is the most common reagent for acid pretreatment methods (Saeman 1945; Herrera et al. 2004; Liu and Wyman 2004; Nilsson et al. 2005; Corredor et al. 2008); although, chloridric and phosphoric acids have also been studied (Herrera et al. 2003; Herrera et al. 2004; Kim et al. 2009). The more diluted the acid solution is, the higher the temperatures need to be get a high yield of glucose during the enzymatic hydrolysis. However, the harsher the conditions are, the less glucose is recovered. Cellulose should remain in its solid phase and its conversion to soluble  $\beta$ -1,4 glucan must be avoided; meanwhile, the lignin and hemicellulose components have to be solubilized. Temperatures in the range of 120 to 220°C are commonly used with this method and the residence time is from a few minutes to 30 minutes, depending on temperature. Increase in temperature improves the sugar yield but increases the glucose degradation. Concentrated acids are used at relatively mild conditions and longer residence times. The sugar yield can be close to the theoretical with concentrated acids, but the cost of the large amounts of acid that is required and the environmental problems associated are a drawback for this method (U.S. Department of Energy 2006).

### ***2.2.2 Alkaline Hydrolysis***

Sodium hydroxide and ammonium hydroxide are the common basic reagents reported in the literature for alkaline pretreatment of biomass (Teymouri et al. 2004a; Kim and Lee 2005; Sun et al. 2005). Alkaline hydrolysis has higher reaction rates than acid hydrolysis or hydrothermolysis (Bobleter 1994). Its major effect is the removal of

lignin from the biomass (Kim and Lee 2005). However, even at temperatures lower than 100°C, basic reagents could react with monomeric sugars such as glucose, fructose, or cellobiose (Yang 1996; Cejpek 2008). Dilute sodium hydroxide works well as a pretreatment driving force because it causes swelling of cellulose, and breaks the crystalline structure and binding forces between lignin and carbohydrates (Deng and Wang 2009).

### ***2.2.3 Hot Compressed Water***

The hot compressed water method uses temperatures higher than 150°C and pressures from 0.1 up to 25MPa. At the pretreatment condition with high temperature and high pressure, water could favor either ionic or free-radical reactions. Subcritical water, or water at temperatures below its critical point and under pressurized conditions, has a greater ionic product (expressed as  $\log [H_3O^+][OH^-]$ ). This fact explains why subcritical water has the properties of an acid or a basic catalyst (Pang et al. 2008). Bobleter et al. (1994) concluded that the mechanism of cellulose degradation with a hydrothermolysis (temperatures about 215-219°C) is similar to that of an acid hydrolysis but with slower reaction rates. Therefore, conditions close to the critical point must be used in order to increase the reaction rates. The high energy input of the process and the high rate of decomposition products at the high temperatures are the disadvantages of this method (Lou et al. 2008).

### ***2.2.4 Steam Explosion***

When treated with the steam explosion method, the biomass is heated and pressurized with steam, and then subjected to a rapid decompression. It has been reported that this method effectively enhances the conversion rate of cellulose into fermentable sugar (Mosier et al. 2002). This pretreatment method is based on the fact that the high temperatures and pressures, plus the rapid decompression to which the material is subjected, can disrupt the plant cell structure. Nonetheless, the catalyst plays an important role (Varga et al. 2004; Datar et al. 2007; Corredor et al. 2008). Varga et al. (2004) showed that the enzymatic hydrolysis of corn stover improves only 3% when the process is carried out at 180°C without acid loading. High sugar yields have been

obtained when acid catalysts plus steam are used (Varga et al. 2004). They reported that corn stover treated at 200°C for 5 min with 2% H<sub>2</sub>SO<sub>4</sub> resulted in the highest enzymatic conversion rate (from cellulose to glucose), which was four times greater than untreated material and up to 73% of the theoretical maximum; meanwhile, they obtained 86% sugar yield when the acid loading to 3 wt.%. At these temperatures, undesired reactions products such as HMF, and formic and acetic acids are also formed, which is the drawback of this method. Viola et al. (2007) reported that the amount of these volatile products increases when the temperature and the acid loading increases.

### ***2.2.5 Ammonia Fiber Explosion***

Ammonia fiber explosion (AFEX) differs from steam explosion in that lignocelluloses are exposed to liquid ammonia instead of water vapor. In a typical treatment, the lignocellulosic materials are treated with high pressure liquid ammonia at 70-100°C for up to 30 min, and then the pressure is quickly reduced. AFEX dramatically increased lignocellulose susceptibility to enzymatic attack in the hydrolysis step. Teymouri et al. (2005) and Viola et al. (2007) optimized the AFEX method for switchgrass, and found that 100°C and 5 min of residence time are the best conditions for its pretreatment. Ninety-three percent of glucan conversion was the maximum yield reached during the enzymatic hydrolysis. In another work (Teymouri et al. 2005), 98% of the theoretical glucose yields were achieved during enzymatic hydrolysis of the optimal treated corn stover. Treatment temperature of 90°C and 5 min of residence time were the optimal conditions for this type of biomass. The same authors reported complete cellulose conversion when they treated DDGS (distiller's dry grains and solubles) with the AFEX method at 70 and 80°C (Teymouri et al. 2004b). The AFEX method was also evaluated with hardwood (Bals et al. 2006). Although 93% yield was achieved, the process required higher temperatures and longer residence times (180°C and 30 min). A major advantage of this method is that the ammonia from the process can be recovered or used as a nitrogen source in the fermentation step. Dale et al. (2009) reported that metabolic yield and the specific ethanol production during

fermentation of pretreated corn stover are enhanced by the degradation products of the AFEX treatment (0.46 g ethanol/g consumed sugars; 0.3 g/L xylitol compared to the complex media 0.43 g ethanol/g consumed sugars; 3.2 g/L xylitol) (Sousa et al. 2009).

### **2.2.6 Supercritical CO<sub>2</sub> Pretreatment**

Supercritical CO<sub>2</sub> pretreatment is a process in which lignocellulosic materials are placed in a pressure vessel with CO<sub>2</sub> at pressures that vary from 120 up to 285 atm for a certain time to allow CO<sub>2</sub> penetration into the lignocelluloses matrix, and then the pressure is rapidly released to flash decomposition reactions. Supercritical CO<sub>2</sub> has the advantage over steam in that the supercritical conditions are reached at low temperatures and pressures: 31°C and 73 atm. Therefore, side reactions such as xylose decomposition can be avoided. Dale and Lau (2009) showed that supercritical CO<sub>2</sub> pretreatment of cellulose Avicel can increase glucose yield by 50%. Kim, K. et al. (2001) reached 85% of sugar yield from hardwood when they treated it at high moisture content (73% w/w). Supercritical CO<sub>2</sub> at 220 atm, 165°C, and 30 min were the conditions for this experiment. Lin et al. (1995) applied this method to the enzymatic hydrolysis of cellulose Avicel and obtained 100% glucose yield. The authors used supercritical carbon dioxide at 120 atm, 50°C for 90 min to achieve these results. Ryu et al. (2001) used both subcritical water and carbon dioxide to treat ginger bagasse starch. The highest degree of hydrolysis (97.1%) was obtained at 200°C for 15 min.

## **2.3 Enzymatic Hydrolysis**

Three different types of cellulases can be used to degrade cellulosic materials: endocellulases, exocellulases, and  $\beta$ -glucosidases. The endocellulases (also called endoglucanases) cleave the polymer chains internally, whereas exocellulases (referred to as exoglucanases) cleave from the reducing and nonreducing ends of the molecule, most often generated by the action of endocellulases. Hence, the endo- and exocellulases work synergistically, and together are required for efficient degradation of cellulose to glucose and cellobiose. The latter is then further cleaved by  $\beta$ -glucosidase.

A mixture of at least three of these enzymes is needed for complete enzymatic hydrolysis of cellulose for biomass conversion. The enzymatic hydrolysis of lignocellulosic materials is relatively slow compared to acid hydrolysis. If biomass was not subjected to a previous pretreatment, the hydrolysis would require high loading of enzymes. In addition, enzymes are also very specific and mild conditions are needed for high enzyme activity and efficiency. At present, high-efficiency enzymes are expensive to produce (Petenate et al. 2004) and their activity can be inhibited by the products of the reaction (Ruth et al. 1999).

## **2.4 Nanocatalyst to Mimic Enzymes**

Enzymes are very complex molecules that decrease activation energy for a specific reaction. These molecules are highly specific for particular reactions. However, the limitations of using enzymes for hydrolysis are expensive and relatively slow reaction, which has led researchers to explore alternatives (catalysts). A lot of research work has been conducted in trying to develop compounds that imitate what enzymes do (Lopezantin et al. 1985).

Some compounds that would potentially work as enzymes do are the self-assembled systems. Cyclodextrines are a good example of self assembled nanoreactors; they are molecules that contain a cavity big enough in which a reaction can take place (Vriezema et al. 2005). Vriezema et al. (2005) also discussed non-covalent systems such as micelle and vesicle-based systems where the cavities or binding sites are formed through reversible and non-covalent interactions. However, macromolecular reactors such as polymers have an advantage above vesicles in that are more stable and rigid.

Other systems receiving a lot of attention for enzyme mimicking are functionalized nanoparticles (Breslow 1995; Mosier et al. 2000; Vriezema et al. 2005; Zheng et al. 2006; Guler and Stupp 2007). Fan et al. (2006) did a mini-review on nanoparticle-supported catalysts and catalytic reactions; gold and magnetic nanoparticles with a large superficial area allow high-capacity loading (Fan and Gao 2006) and because the domain sites are usually bound to the surface, the reactants can easily reach the active sites. Gold and magnetic nanoclusters can also be easily

recovered by centrifugation or applying a permanent magnet. The catalysts are usually anchored to the magnetic nanoparticles as a layer of organic coatings using silanes or ethenediols (McCarty and Weiss 1999). Gold and magnetic particles are basically carriers; they don't directly promote the reaction. The particles can hold up heavy metal complexes, organic catalysts, enzymes, and biomimetic catalytic species. The gold species have a monolayer of long-chained alkanethiols, with an SH- or -S-S- terminus, that are linked to the catalyst. Another advantage of using functionalized nanoparticles is that the dispersion can have a solution-like behavior. With proper selection of ligand functionality and solvent, single-crystal nanoparticles with controlled diameters (typically 1-10nm) can be made to behave like molecular solutions (as compared to colloidal solutions that require stabilization via dispersion) (Hyeon 2003).

#### ***2.4.1 Acid-Supported Materials***

Because of environmental issues associated with use of homogeneous acids, such as sulfuric and fluorhydric acid catalysts, development of heterogeneous acid catalysts is receiving a lot of attention (Kim et al. 2005). Homogeneous catalysts have recently been replaced by acid supported catalysts due to recovery advantages. A heterogeneous catalyst can be made by physical or covalent attachment of the active molecule to a support. Preparation of the catalyst usually requires modification of the support to make it able to host the moieties that contain either active sites or specific functional groups. These procedures could demand dedicated organic synthesis; therefore, the catalyst must be reusable many times to balance this difficulty (Hart et al. 2002; Alvaro 2005; Rac et al. 2006; Bootsma and Shanks 2007; Harmer et al. 2007).

#### ***2.4.2 Acid Functionalization of Silica***

MCM-41 and SBA-15 are the most common silica mesoporous structures available in the market. Their porous structures allow them to host molecules with particular functional groups. In general, these porous structures have a mildly acidic activity (Corma and Garcia 2006). In order to increase the acid activity of these structures, acid sites can be added to the surface. For example, the synthesis of MCM-

41/SO<sub>3</sub>H or SBA-15/ SO<sub>3</sub>H can be achieved by linking a precursor and a tetraalkoxyane such as tetraortosilicate TEOS with mercapto groups such as MPTMS (3-mercaptopropyltrimethoxysilane) and CSPTMS (2-(4-chlorosulfonylphenyl)ethyltrimethoxyane) that are oxidated later. This method is known as co-condensation (Corma and Garcia 2006; Margelefsky et al. 2007). MCM-41/SO<sub>3</sub>H has been used for esterification of fatty acids and organic alcohols among other reactions (Corma and Garcia 2006; Rac et al. 2006). Corma and Garcia (2006) also prepared and evaluated the performance of MCM-41 functionalized with perfluoroalkyl-sulfonic acid groups. The catalysts were tested in the esterification of long-chain fatty acids with ethanol and conversion rate up to 95% was reached. Figure 2-2 shows how the acid groups attached to silica surfaces.

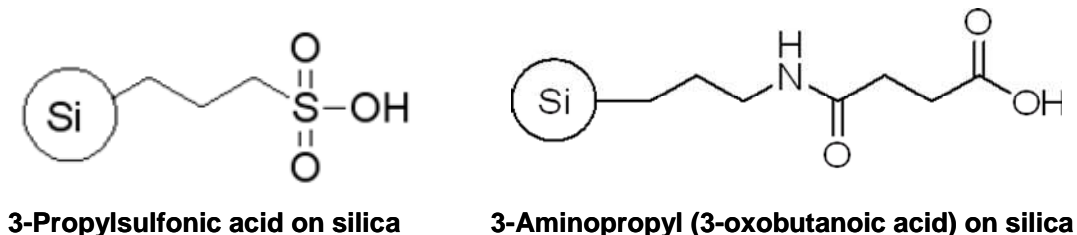


**Figure 2-2 Acid-functionalized silicas representation**

### **2.4.3 Silica-Supported Perfluoroalkyl-sulfonic Acids**

Nafion has been reported as one of the most important examples of an insoluble strong acid (Alvaro et al. 2005) (Figure 2-3). It is a perfluoroalanesulfonic acid and contains about 15-20 mol% of sulfonic groups. Even though it is a strong and stable acid, it has a small surface area. Nafion has no permanent porosity and swells slowly and relatively little in most polar solvents (Corma and Garcia 2006; Siril et al. 2007).

In order to increase the area and improve the catalytic activity, Nafion was anchored to MCM-41. This new composite is called Nafion@MCM-41. Nafion@MCM-41 was used for the catalytic esterification of carboxylic acids. The method by which it was attached to MCM-41 is called the grafting approach (Siril et al. 2007). Nafion@MCM-41 has the advantage that it can increase the acid site accessibility. However, it has limited stability. Starting with a pre-formed support, such as MCM-41, could have some hindrances because the Nafion resin is a fine colloidal dispersion and the polymer can't penetrate effectively within the internal pores of the support. The polymer could remain

as micron lumps on the outer surface of the support according to Harmer et al. (2000). The authors recommend the *in-situ* approach sol-gel method because of the improved dispersion, higher effective surface area of the Nafion, and improved stability. Harmer et al. (2000) also recommend using silicon alcoxides as the precursor rather than sodium silicate as the silica source when a highly dispersed Nafion in silica system is required.

Siril et al. (2007) compared the catalytic activity of sulfonic acid on polymeric and silica supports. The nafion-functionalized silica SAC-13 gave better results than Amberlyst, arylsulfonic and propylsulfonic acids, and even Nafion pellets. The better performance of Nafion SAC-13 was explained because of the accessibility of the acid sites due to its dispersion on a nanometer scale (Harmer et al. 1998). Harmer et al. (1998) also affirmed that Nafion silica nanocomposites have the solid-acid properties of Nafion resin and physicochemical properties of silica such as high surface area, and mechanical and thermal stability.

On the other hand, the affinity of the catalyst surface and the reaction medium strongly influence the performance of silica-supported sulfonic acids. Therefore, the hydrophilicity of these solids acids made them adequate for reactions in polar mediums. (Siril et al. 2007) affirmed that resins containing acid groups such as Nafion are strong enough to protonate water. (Harmer et al. 1998) evaluated the performance of silica-supported Nafion as catalyst on the removal of methyl tert-butyl ether (MTBE) from water. The authors reached separation efficiency up to 70%. However, the transformation accounted just 18% of the MTBE lost. Lien and Zhang (2007) also affirmed that after 10,000 turnovers the catalyst become darker in color and lose activity. According to their reported results, the catalysts can be recovered using nitric acid of 25 % (wt) at 50°C for 4h.

The amorphous silica-supported acids have reaction limitations in the liquid phase. A dispersed system is necessary to increase their reaction activities and types of reactions. Fortunately, acids groups can be attached to disperse nanoparticles. Jones and his research group have developed a method to bind acid groups to silica-coated magnetic nanoparticles (Harmer et al. 2000). The magnetic core is first synthesized and then coated with a silica layer. This layer is later functionalized with acid groups in a similar way as mesoporous silica is functionalized (Gill et al. 2007).

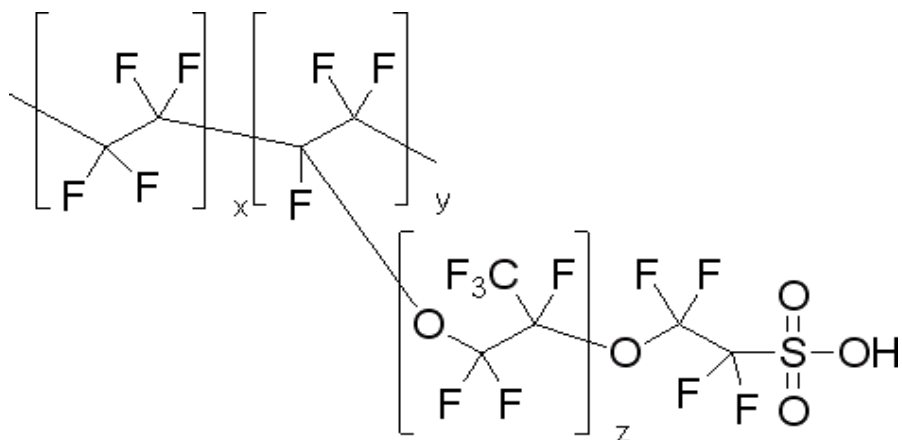


**Figure 2-3 Fluorosulfonic acid resin Nafion® SAC-13**

#### **2.4.4 Acid Strength of Sulfonic Supported Acids**

Some authors have used ion exchange titrations for determination of the acid loading capacity of sulfonated resins through ion exchange titrations (Phan and Jones 2006; Gill et al. 2007). Table 2-1 shows some of the values reported in the literature for some solid acids. Acid loading is expressed as the concentration of the hydronium ion in solution. The protons in the acid sites are exchanged for the cations in a salt solution; the protons are expelled to the solution and counted through titration with a basic solution. This value is the total amount of acid sites available in the material. However, in aqueous solutions, the amounts of dissociated protons depend on the ion exchange capacity of the particular media. Some of the protons might remain in the associate state and some others would go to the solution. The acid strength of solid acid composites also can be measured by the determination of the molar enthalpies of neutralization and by ammonia adsorption calorimetry (Hart et al. 2002; Melero et al. 2002). Hart et al. (2002) found that the acid strength of hydrated and dehydrated sulfonic functionalized resins increases with the degree of sulfonation. The authors also observed that the catalytic activity was increased as the water content decreased. Diminution of the acid strength is expected in the presence of water because of the dissolution of the hydro-ion, whose acidity is not as strong as that of the sulfonic group. However, an increase in the molar enthalpy of neutralization was found. The enhanced acid strength in the presence of water was explained as the higher acid concentration in

the hydrated resin that leads the acid groups to the associated state. In order to improve the acid strength of acid solid supported materials, some studies have been reported on the attachment of perfluoroalkyl-sulfonic acid groups upon mesoporous silica (Hart et al. 2002; Siril et al. 2007). The increase in the acid strength of the sulfonic group is attributed to the electron withdrawing properties of the F atoms (Harmer et al. 1998; Corma et al. 2004).

**Table 2-1 Acid loading of some solid acids**

	Functional group	Acid sites (mmol/g)
Activated carbon	nd	1.25 <sup>a</sup>
Activated carbon/SO <sub>3</sub> H	SO <sub>3</sub> H	1.63 <sup>a</sup>
Sulfated zirconia	SO <sub>3</sub> H	1.60 <sup>a</sup>
Amberlyst 15	SO <sub>3</sub> H	1.8 <sup>a</sup>
Amberlyst-15	SO <sub>3</sub> H	4.65 <sup>b</sup>
Nafion-SAC13	FSO <sub>3</sub> H	0.17 <sup>b</sup>
H-modernite	Acidic OH	0.7 <sup>c</sup>
Si-MPTMS nanoparticles	SO <sub>3</sub> H	0.47 <sup>d</sup>
Si-FSO <sub>3</sub> H nanoparticles	SO <sub>3</sub> H	0.78 <sup>d</sup>

Data from <sup>a</sup> Corma et al. (2004), <sup>b</sup> Onda et al. (2008), <sup>c</sup> Dhepe et al. (2005), <sup>d</sup> Fukuoka and Dhepe (2006)

## 2.5 Solid Supported Acids for Cellulose Hydrolysis

Homogeneous acids have been used effectively for pretreatment of lignocellulosic materials that would be later degraded to sugar monomers for ethanol production. At present, lignocellulosic alcohol is not yet economically feasible (Gill et al. 2007). Regular inputs of catalyst and continuous disposal of waste material are substantial costs of the process. The recoverability of solid acid supported systems makes them a suitable alternative for their homogeneous counterparts. In this area, some preliminary studies have been conducted (Allred et al. 2008; International Trade Commission and Jim Jordan and Associates 2009; Van Dyne et al. 2000). Dhepe et al.

(2005) used water tolerant sulfonated silicas to break the  $\alpha$ -1,2 glycosidic bond between the glucose and fructose units in the sucrose molecule, and yields of up to 90% were obtained. The  $\alpha$ -1,4 glycosidic bond in starch was also subjected to hydrolysis but the glucose yields barely reached 40%. In a different approach, Shanks et al. (2007) used acid-functionalized mesoporous silica as catalyst to break  $\beta$ -1,4 glycosidic bonds in the cellobiose. Glucose yields up to 90% were reported for some of the functionalized silicas. Cellulose has also been hydrolyzed with acid sulfonated carbon. Some authors have reported the treatment of treated microcrystalline cellulose with sulfonic acid-functionalized amorphous and activated carbon; glucan yields of 64% and 45% were obtained (Bootsma and Shanks 2007). Besides microcrystalline cellulose, Suganuma et al. (2008) hydrolyzed eucalyptus flakes and got conversion rates higher than 90% (Figure 2-4). Other substrates such as cellulose and cellobiose have also been evaluated and the previous reported results are summarized in Table 2-2.

To increase the contact area between mesoporous materials and substrates for high conversion yield and efficiency, the present work proposes use of acid-functionalized nanoparticles for treatment of cellulosic materials.

**Table 2-2 Glucose yields from oligosaccharides using solid acid catalyst**

Catalyst	Substrate	Temperature (°C)	Glucose yield (%)	Time (h)
AC-SO <sub>3</sub> H <sup>a</sup>	Cellobiose	90	80	24
Amberlyst <sup>a</sup>	Cellobiose	90	60	24
AC-SO <sub>3</sub> H <sup>a</sup>	Cellohexaose	90	80	15
AC-SO <sub>3</sub> H <sup>b</sup>	Cellulose	150	40.5	24
AC-SO <sub>3</sub> H <sup>c</sup>	Cellulose	100	4 (glucan 64)	3
H <sub>2</sub> SO <sub>4</sub> <sup>c</sup>	Cellulose	100	10 (glucan 38)	3
Amberlyst-15 <sup>c</sup>	Cellulose	100	0	3
Nafion <sup>c</sup>	Cellulose	100	0	3

(Adopted from <sup>a</sup> Kitano, 2009; <sup>b</sup> Onda 2008; <sup>c</sup> Suganuma 2008)

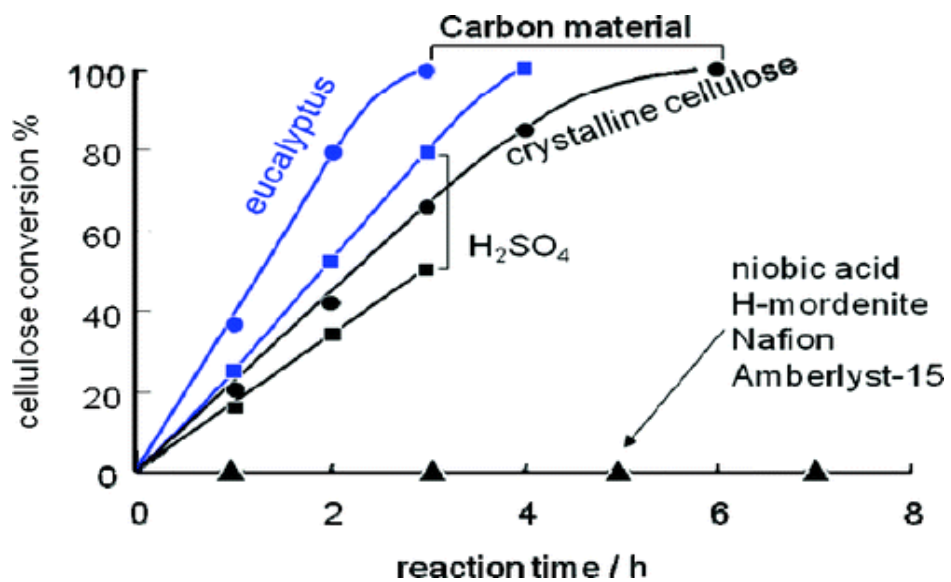


Figure 2-4 Cellulose Conversion using amorphous carbon with sulfonic groups (Adopted from Suganuma et al. 2008).

# CHAPTER 3 - Synthesis and Characterization of Acid-functionalized Magnetic Nanoparticles

## 3.1 Introduction

Strong mineral acids such as sulfuric and fluorhydric acid are commonly used as catalysts in oil refining and chemical synthesis (Albright 1990; Martinez and Corma 1993; Rhodes 1994). The chemical waste of these processes contaminates surface water sources and decreases air quality. SO<sub>2</sub> emissions and acidic water streams derivated from the production and utilization of sulfuric acid create serious environmental problems such as acid rain, acidification of the soil, and reduction of the amount and diversity of aquatic species (U.S EPA 1984; Van Vuuren 2002; Orisakwe 2008; Zhang 2008; Richardson 2009;, Taniyasu 2009; Ward 2009). Environmental and safety concerns have stimulated the research on solid supported acid as an alternative for homogeneous catalysts. Zeolites (aluminosilicate), amberlytes (resine), sulfated zirconia, and perfluorinated resin sulfonic acids are already available on the market. Extensive studies have also been reported on the synthesis and evaluation of mesoporous silicas functionalized with acid groups (Harmer et al. 1996; Harmer et al. 1998; Van Rhijn 1998; Corma et al. 2004; Alvaro 2005; Rac et al. 2006; Harmer et al. 2007). Van Rhijin et al. (1998) synthesized MCM with covalent attachment of alkyl-sulfonic acid groups. The MCM-SO<sub>3</sub>H was used to catalyze the formation of bisfurylalkanes and polyol esters. Catalysis of reactions such as alkenes isomerization, alkylation, and acylation with perfluoroalkyl-sulfonic acids attached on silica supports were reported by Harmer et al. (1997). In another work, Melero et al. (2002) produced SBA-15 mesoporous silica containing arenesulfonic acid groups; the material was reported to be stable to temperatures up to 380°C and resistant to leaching in aqueous solutions. Nevertheless, acid-functionalized mesoporous silicas possess a limited accessibility of the reagents to the active sites.

Monodisperse materials have an advantage that provides large surface areas. Several studies can be found on supported acid groups linked to disperse materials (Li 2003; Fiurasek 2007; Gill 2007). Monodisperse materials such as nanoparticles have a

great potential for developing heterogeneous catalysts with the dispersion capability of their homogeneous counterparts. In general, the nanoparticles have a large superficial area that provides a high reaction rate between the reagents and the acid groups.

The word nanoparticle is the term applied to materials whose size is too small that the system can't be well described by common Newtonian physics. On the other hand, nanoparticles are not small enough to be considered as belonging to the molecular scale, so they can not be explained by quantum mechanics (Roukes 2001). New physical and chemical properties are being revealed for certain materials when their size is at the nanometer scale. Surface chemistry is enhanced because the increase in surface area allows better contact with other reagents, metals improve their hardness, and ceramics increase their ductility and plasticity (Averback 1989; Li 1993; Utamapanya 1993). Elements such as Na and Li show nonmetallic behavior in the nanoscale. Conductivity of these materials decreases as size decreases due to the expansion of the band gap; in this instance, their nanoscale counterparts can be used as insulators (Rogers 2008). Optic and magnetic behaviors, as well as thermodynamic properties like melting temperatures and coordination numbers, can also change with size (Van Sicle 2007; Nanda 2009). Nanomaterials have drawn a lot of attention because their particular characteristics may allow development of new applications; desired properties can be attained by means of tuning of the size of the material.

Among the magnetic properties, superparamagnetism is the one that has attracted the most attention in the biological and biomedical areas (Pankhurst 2003; Bromberg 2005). Superparamagnetic materials respond effectively when exposed to a magnetic field, but they retain no remnant magnetization when the magnetic field is removed. Magnetic materials such as  $\text{MgFeO}_4$  and  $\text{CoFeO}_4$  have superparamagnetic behavior when their size is at the nanometer scale (Chen, 1998; Calero-DdelC 2007).

Extensive research has been done on the use of homogeneous acids such as sulfuric, chlorhydric and phosphoric acids for the pretreatment of biomass for subsequent ethanol production (Hashimoto 1997; Herrera, 2004; Liu 2004; Viola 2007; Kim 2009). Acid-functionalized nanoparticles may have potential as catalysts for pretreatment and hydrolysis of lignocellulosic biomass. Using magnetic acid-functionalized nanoparticles would potentially provide the hydrolytic benefits of the acid

solutions with the advantage that they can be recovered and reused. Jones et al. (2007) developed a method to synthesize acid-functionalized magnetic nanoparticles. This method is applied in the present work to synthesize two different catalysts. Cobalt spinel ferrite ( $\text{CoFeO}_4$ ) nanoparticles are first synthesized by a microemulsion method (Rondinone 1999). In order to prevent oxidation and to facilitate further functionalization, the magnetic nanoparticles are coated with a silica layer (Zhang 2008). In the final step, the silica-coated magnetic nanoparticles are functionalized with alkyl-sulfonic and perfluoroalkyl-sulfonic acids. Therefore, the objectives of this research are to synthesize the cobalt spinel ferrite magnetic nanoparticles functionalized with acid functions using sulfonic and perfluoroalkyl-sulfonic acids and to characterize the acid-functionalized nanoparticles in terms of particle size, acid functional groups, and pH.

## **3.2 Materials and Methods**

### **3.2.1 Chemicals**

Ammonium hydroxide (Fisher Scientific, A.C.S. reagent), D-(+)-Cellobiose (Sigma-Aldrich, 98%), cobalt (II) chloride tetrahydrate (Riedel-deHaën, 99%), diethylamine (Sigma-Aldrich, 99.5%), ethanol (Pharmco-AAPER, 95%), iron (II) chloride (Sigma-Aldrich, 99.99%), hexafluoro (3-methyl-1,2-oxathiane)-2,2-dioxide (HFP sultone) (SynQuest Labs, 95%) and isopropanol (Fisher Scientific, A.C.S. reagent), 3-mercaptopropyltrimethoxysilane (MPTMS) (95%, Aldrich), methylamine (40%w/w Sigma-Aldrich 98.5%), sodium dodecyl sulfate (Sigma-Aldrich, 98.5%), tetraethylorthosilicate (TEOS) (Sigma-Aldrich, 99.999%), and toluene (Fisher Scientific, A.C.S. reagent) were used as raw materials for synthesizing acid-functionalized nanoparticles.

### **3.2.2 Sonication**

A sonication bath (VWR Scientific P250D) was used for the silica-coating process before the acid functionalization and previous to the biomass hydrolysis.

### **3.2.3 TEM Images**

Transmission electron microscope (TEM) images were used to estimate the size and distribution of particles at the nanoscale level. A model FEI CM100 TEM (FEI Company, Hillsboro, Oregon, USA) equipped with an AMT digital image capturing system was operated at 100 kV. The images were taken under both dispersed and dried conditions. For dispersed solutions, the nanoparticles were absorbed for approximately 30 s at room temperature onto Formvar/carbon-coated, 200-mesh copper grids (Electron Microscopy Sciences, Fort Washington, Penn., USA), and then viewed by TEM.

### **3.2.4 FTIR Analysis**

Fourier transform infrared (FTIR) spectra were used to investigate the chemical composition of the synthesized nanoparticles. Chemical bonds of the compounds in the sample absorb infrared light at very specific frequencies. The infrared light is partly reflected from the surface and partly transmitted to a depth of a few micrometers in powdered material. The light that enters the material is absorbed or scattered. The re-emitted light has components from the surface and layers close to the surface. This phenomenon, in which the light is reflected in many different directions, is termed diffuse reflectance. Reagent KBr and samples were dried for 24 h at 103°C and then prepared by mixing 2 mg of sample with 200 mg of spectroscopy grade KBr. The measurement was carried out in the wave number range 400 – 4000  $\text{cm}^{-1}$ , with detector at 4  $\text{cm}^{-1}$  resolution and 32 scans per sample using a Thermo Nicolet NEXUS™ 870 infrared spectrometer (Spectra-Tech: Model No. 0031-901) with a ZnSe window. An OMNIC software program by Nicolet was used to determine the peak positions and intensities.

### **3.2.5 Preparation of Magnetic Nanoparticles (MNPs)**

Cobalt spinel ferrite ( $\text{CoFe}_2\text{O}_4$ ) nanoparticles were synthesized using the microemulsion method previously described in the literature (Phan and Jones 2006; Rondinone 1999; Gill 2007). In a typical experiment, 0.9g of cobalt (II) chloride and 1.9 g of iron (II) chloride were mixed to form an aqueous solution (500ml). Twelve and nine-tenths grams of sodium dodecylsulfate (SDS) were dissolved in distilled water to

complete 500ml of solution. This solution was added to the cobalt and iron solution. The mixture was stirred at room temperature with a mechanical stirrer for 30 min, and then heated to 58°C. Another solution was prepared with 300 ml of methylamine (40% w/w) and distilled water to complete 1L of solution and was heated to 58°C, too. Both solutions were finally mixed and stirred for 3 h. The nanoparticles were separated magnetically and then washed three times using distilled water. Then 100 ml of ethanol were used for a final rinse.

### **3.2.6 Silica Coating of the Magnetic Nanoparticles (SiMNPs)**

The silica coating procedure was carried out following the method described previously by Gill et al. (2007). The ethanol dispersion of nanoparticles was sonicated and stirred simultaneously for 30 min; after sonication 12 ml of the solution were mixed with 522 ml of isopropanol and 40 ml of water. This solution was also sonicated under mechanical stirring for 1h. Then, 47 ml of concentrated ammonium hydroxide were added to the mixture. A solution 1 ml of tetraethylorthosilicate (TEOS) in 40 ml of isopropanol was added dropwise to the former solution over a 1-h period under mechanical stirring. The mixture was again sonicated under mechanical stirring for 1h. The nanoparticles were washed with large amounts of water and separated out of the solution using a permanent magnet. The nanoparticles were dried in an air-force oven at 103°C for 24 h. About 250 mg of the product was obtained.

### **3.2.7 Acid Functionalization of the Silica-coated Magnetic Nanoparticles**

**Preparation of supported alkyl-sulfonic acid (AS-SiMNPs):** The alkyl-sulfonic acid function upon the silica-coated nanoparticles was carried out following the procedure described by Gill et al. (2007) (Figure 3-1). A solution with 1 g of MPTMS, 10 ml of ethanol, and 10 ml of water was prepared. Then, 250 mg of SiMNP were added. The mixture was sonicated for 15 min and refluxed overnight. SiMNP-SH were recovered magnetically and washed three times with 50 ml of water. A solution of 10 ml of 30% hydrogen peroxide, 10 ml of water, and 10 ml of methanol was added to the recovered SiMNP-SH and left overnight at room temperature. The product of the oxidation step was recovered magnetically and washed three times with 20ml of water.

The particles were reacidified with 10ml of 1M H<sub>2</sub>SO<sub>4</sub>, washed three times with water, recovered magnetically, and dried in an air-forced oven at 40°C for 24h.

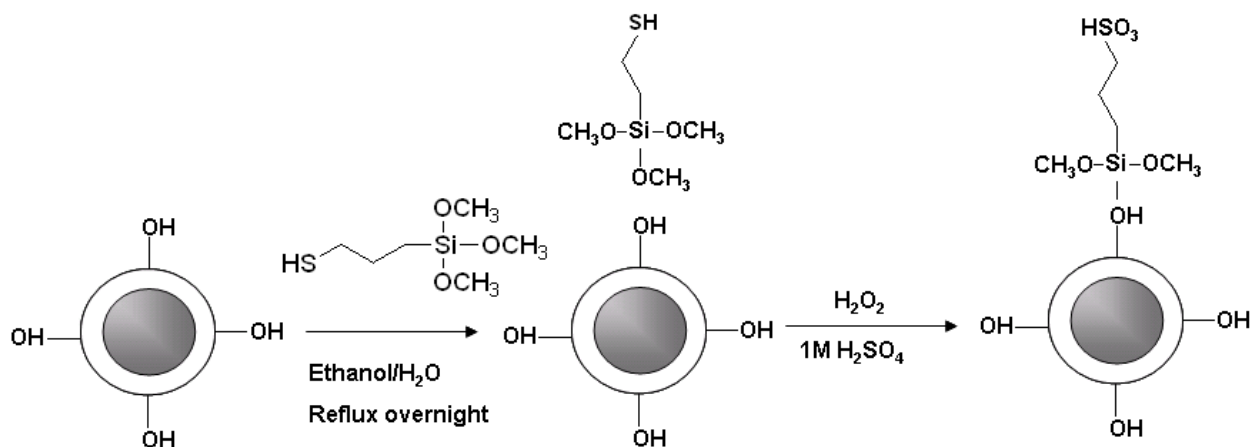


**Figure 3-1 Schematic representation for AS-SiMNPs preparation (Adopted from Gill et al. 2007)**

**Preparation of supported perfluoroalkyl-sulfonic acid (HPS-SiMNPs):** The perfluoroalkyl-sulfonic acid function upon the SiMNPs was produced by following the procedure described by Gill et al (2007). Two hundred and fifty mg of SiMNPs, dried at 110°C overnight, were placed in a 125-ml pressure bottle. One ml of HFP SULTONE and 20 ml of anhydrous toluene were poured into the bottle in a nitrogen glove bag. The pressure bottle was sealed and sonicated for 20 min. The mixture was stirred at 100°C for 4 h in a waterbath. The fluoro-sulfonic-acid product (SiMNPs-FSO<sub>3</sub>H) was washed three times with 20 ml of anhydrous toluene and recovered magnetically. The nanoparticles were dried at room temperature overnight. Figure 3-2 shows the procedure of preparation of HPS-SiMNPs.

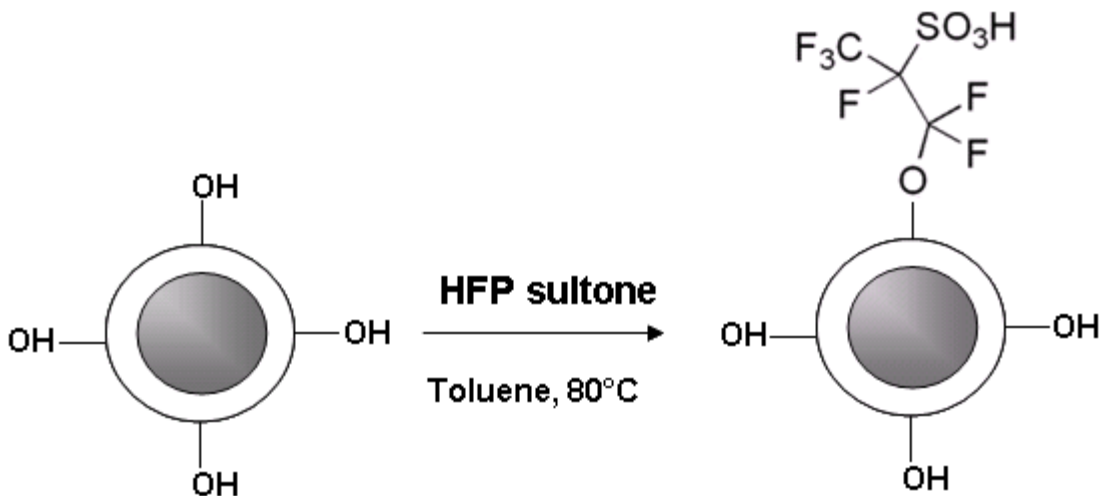


Figure 3-2 Schematic representation for HPS-SiMNPs preparation (Adopted from Gill et al. 2007)

### 3.4 Results and Discussion

#### 3.4.1 Particles Size and Distribution of Synthesized Nanoparticles

##### 3.4.1.1 Particle Size of Cobalt Spinel Ferrite

Figures 3-3 and 3-4 are the images taken of a disperse solution of cobalt spinel ferrite nanoparticles in ethanol. Well-dispersed nanoscale particles can be observed. The range of particle size is from 5.3 nm to 11.0 nm in these images.

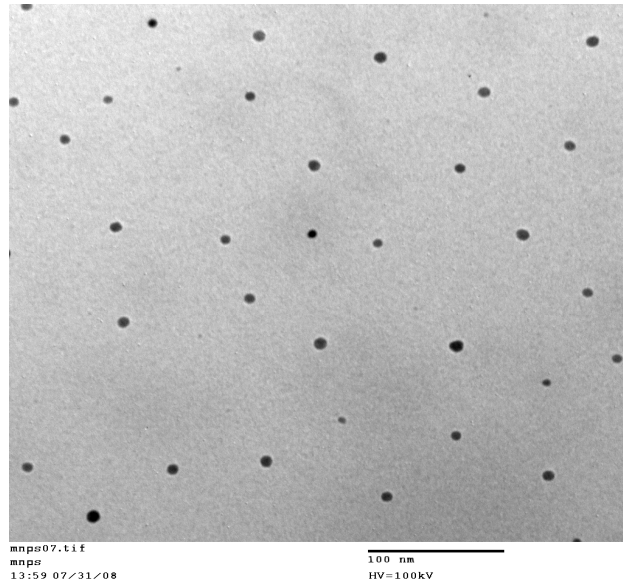


**Figure 3-3 Cobalt spinel ferrite nanoparticles (100 nm scale)**

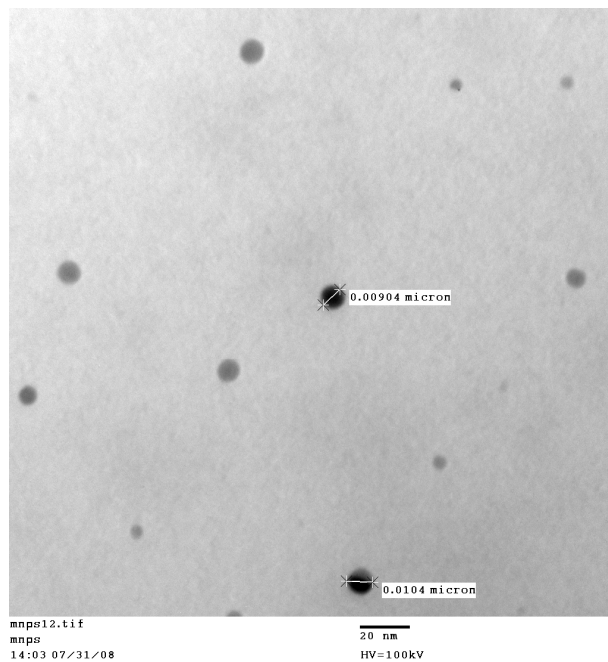
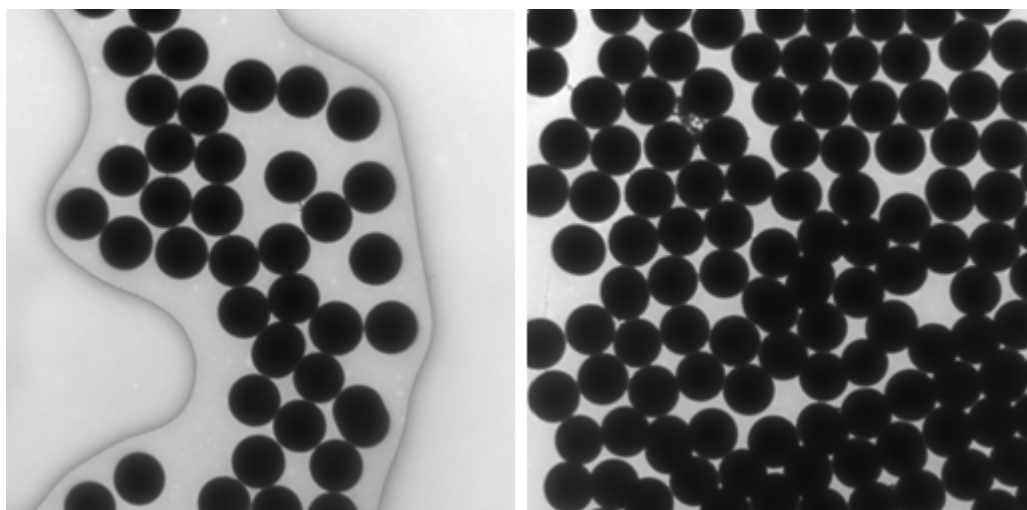


**Figure 3-4 Cobalt spinel ferrite nanoparticles (20nm scale)**

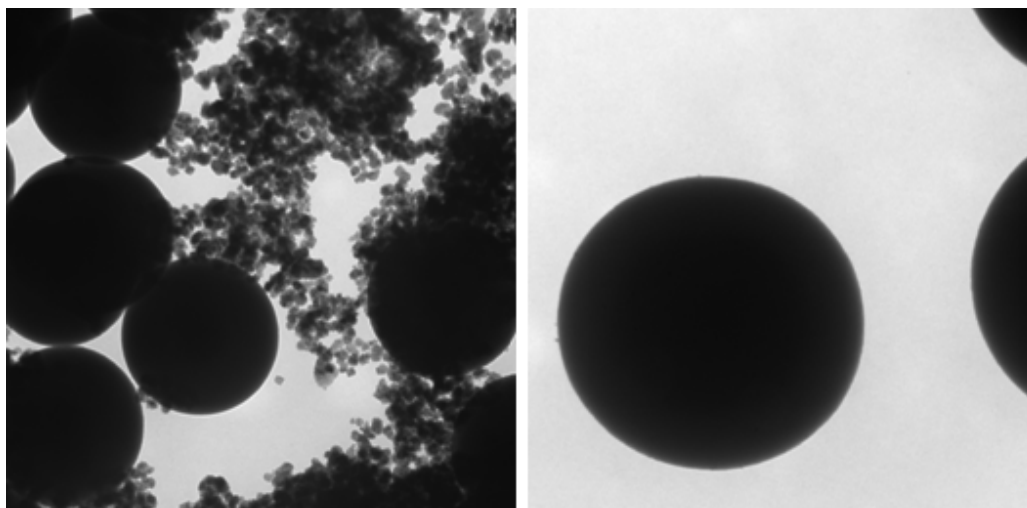
### **3.4.1.2 Particle Size of Silica-coated Nanoparticles**

Figures 3-5 and 3-6 show the images of silica-coated particles. The silica coating process is quite sensitive to the TEOS concentration in the solution. Size of the silica

layer was significantly affected by the TEOS concentration in the solution (Zhang 2008). In this case, if the TEOS solution was added too fast, then particle sizes could be up to 500 nm (Figure 3-5). The perfectly round shape of the particles may be an indicator that individual particles, rather than clumps, were obtained. In Figure 3-6, material of a smaller size can also be observed.



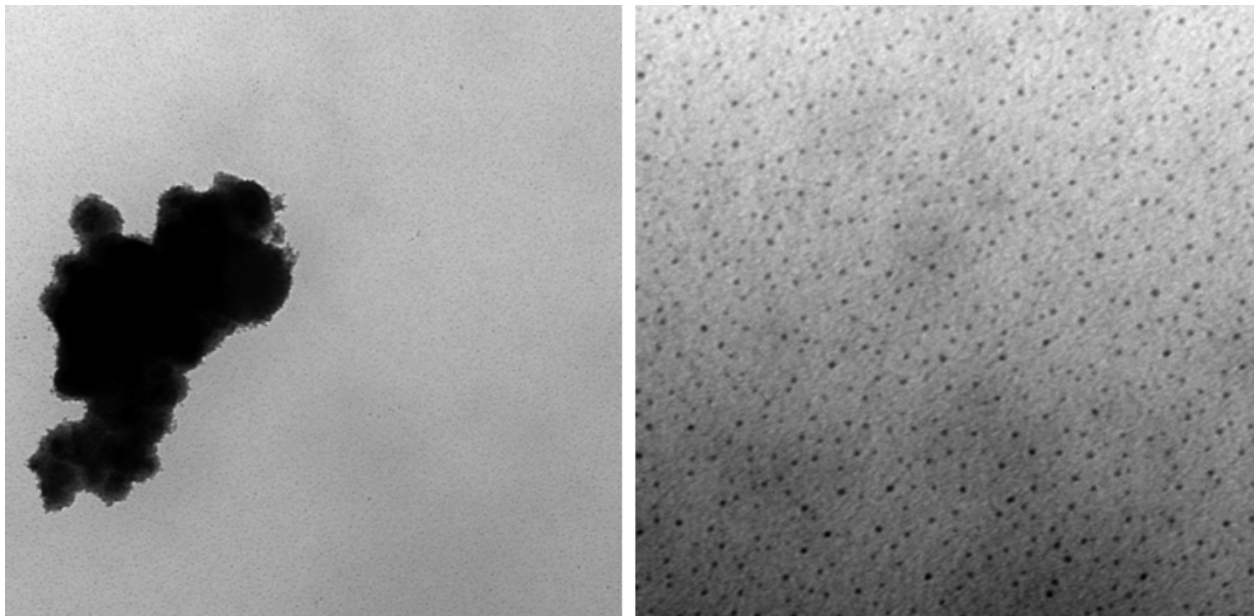
**Figure 3-5 Silica-coated cobalt spinel ferrite nanoparticles (500 nm scale)**



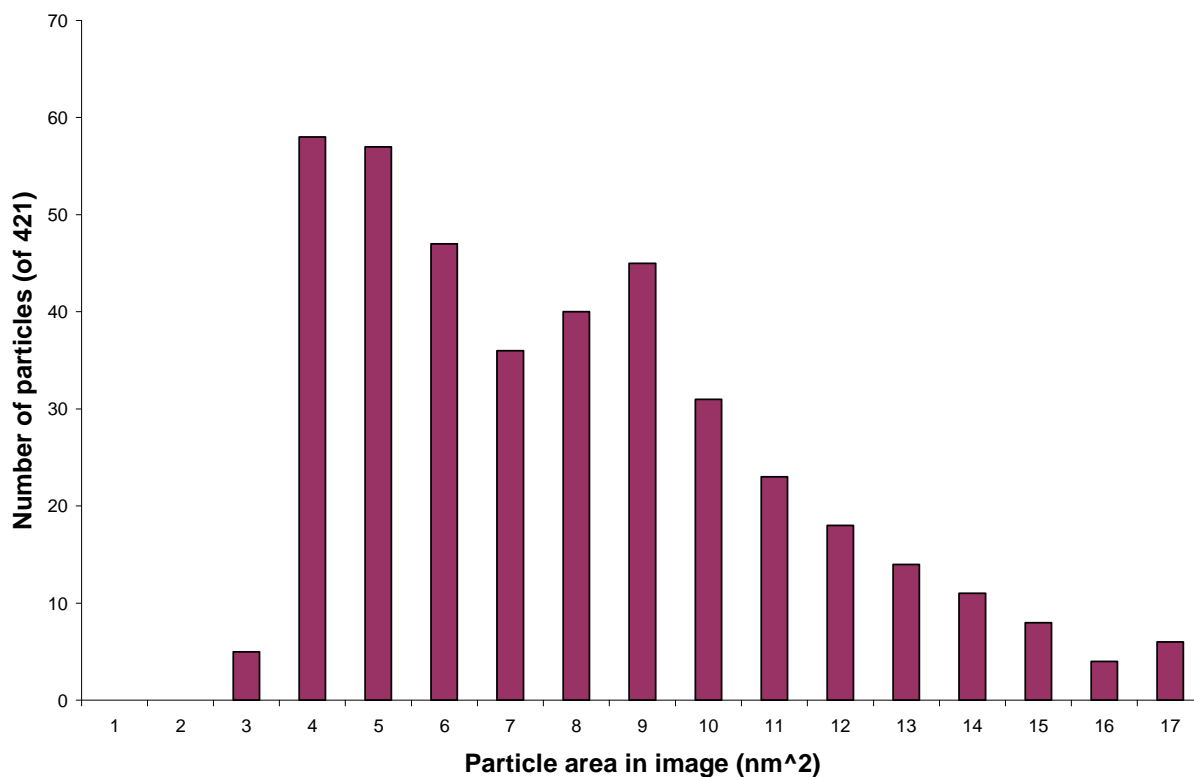
**Figure 3-6 Silica-coated cobalt spinel ferrite nanoparticles (100 nm scale)**

Figure 3-7 shows the images of silica-coated cospinel ferrite nanoparticles. The images were taken upon bench-top-dried samples. Some clumps can still be seen (right

side of the figure). In order to get silica layers in the nanoscale, the TEOS solution was added upon the dispersion of cobalt spinel ferrite nanoparticles. Sizes of silica-coated particles were all in the nanoscale range. Average area of the nanoparticles was found to be  $4.54 \text{ nm}^2$  (assuming spherical shape), and the average diameter of the nanoparticles was 2.4 nm based on an average of 400 nanoparticles. The standard deviation of the particles area was  $2.14 \text{ nm}^2$  and the size distribution can be seen in Figure 3-8. Although the standard deviation is relatively large, most of the particles have an area less than  $15 \text{ nm}^2$  and maximum size of the particles is 4.4 nm.



**Figure 3-7 Silica-coated cobalt spinel ferrite nanoparticles (left, 100 nm scale; right, 20 nm scale)**



**Figure 3-8 Histogram for silica-coated nanoparticles**

### **3.4.1.3 Particle Size of Acid-functionalized Nanoparticles**

Perfluoroalkyl-sulfonic acid nanoparticles: Figure 3-9 shows the TEM images of the perfluoroalkyl-sulfonic acid nanoparticles. Some of the particles have more than one small core nanoparticle. This indicates there were some aggregated particles either during the coating with silica or during the functionalization of the particles. However, size of the particles remains in the nanoscale, and ranges between 2.0 nm to 12 nm.

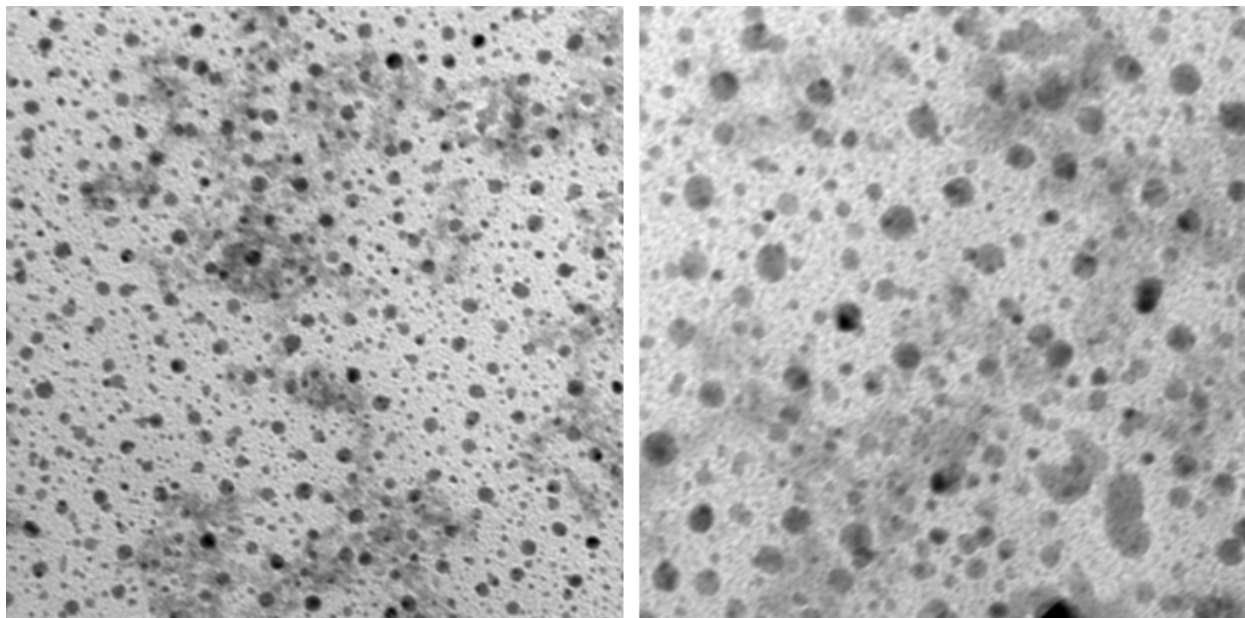


**Figure 3-9 Perfluoroalkyl-sulfonic acid nanoparticles (left, 100 nm scale; right 20 nm scale)**

**Alkyl-sulfonic acid nanoparticles:** Figure 3-10 shows images of the alkyl-sulfonic acid nanoparticles, well dispersed in the aqueous solution. The size distribution remained in the nanoscale after the coating and functionalization processes. The average area of the nanoparticles was found to be  $37.5 \text{ nm}^2$  (assuming spherical shape) and the average diameter was 6.9 nm based on average of 600 nanoparticles. The standard deviation of the particles area was  $36.4 \text{ nm}^2$  and the size distribution is shown in Figure 3-11. Although the standard deviation is relatively large, the maximum size of the nanoparticles is only 19.3 nm. We believe that this size is good enough to allow good contact between the acid sites and the substrate that is going to be hydrolyzed.

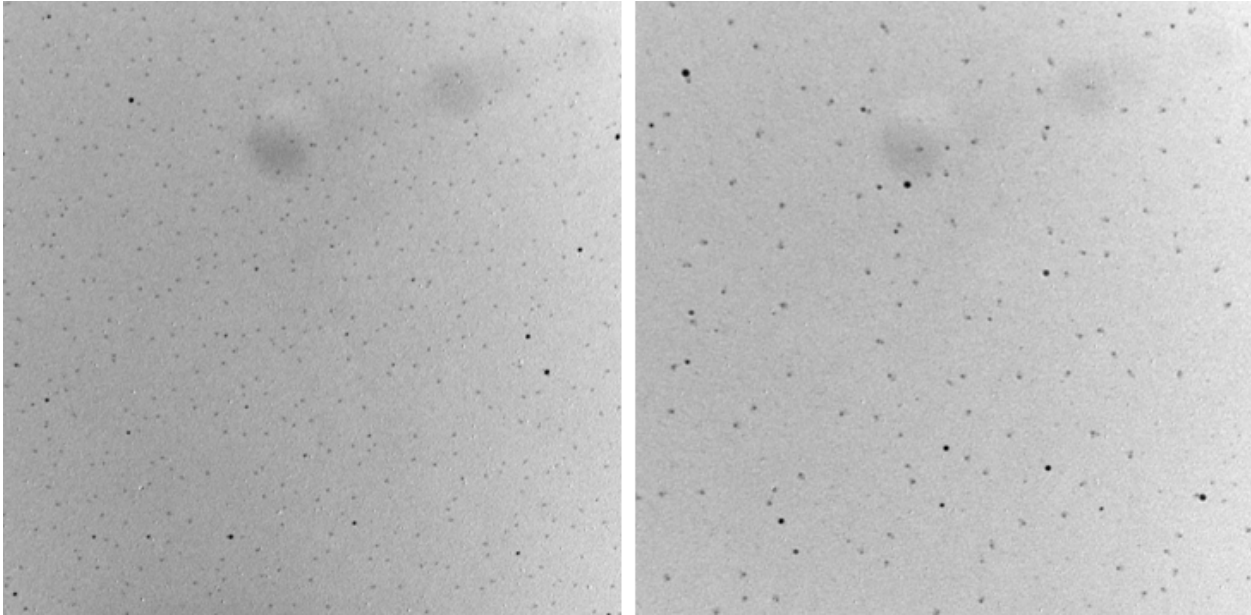


**Figure 3-10 Alkyl-sulfonic-acid nanoparticles (100 nm scale)**

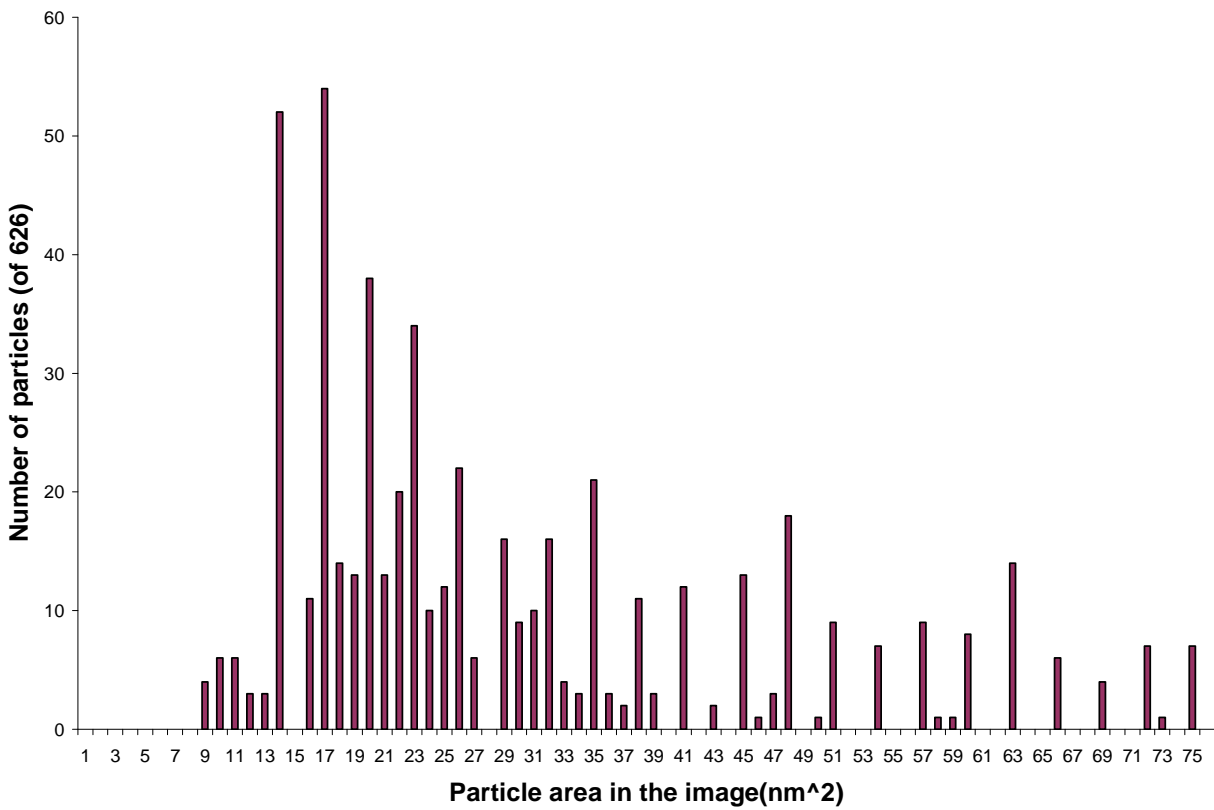


**Figure 3-11 Histogram for the AS-SiMNPs**

### 3.4.2 FTIR Spectrum

FTIR spectra for the acid-functionalized nanoparticles are shown in Figures 3-12, 3-13 and 3-14. The peak at  $3390\text{ cm}^{-1}$  in all spectra could be attributed to the O-H stretching vibrations of physisorbed water and possibly surface hydroxyls. The peak near  $1620\text{ cm}^{-1}$  has been attributed to an O-H deformation vibration (Phan and Jones 2006). Those peaks are shown in the FTIR spectra for the silica-coated nanoparticles (Figure 3-12), the AS- SiMNP (Figure 3-13) and the PFS-SiMNP (Figure 3-14). Phan et al (2006) also point out the peaks at  $1017\text{ cm}^{-1}$  of the Si-O stretching clearly distinguished in the AS- SiMNP (Figure 3-13) and the PFS-SiMNP (Figure 3-14). According to Zhao et al. (2000), the peaks at  $810$  and  $980\text{ cm}^{-1}$  could be attributed to the stretching vibrations of Si-O-Si and Si-O-H groups.

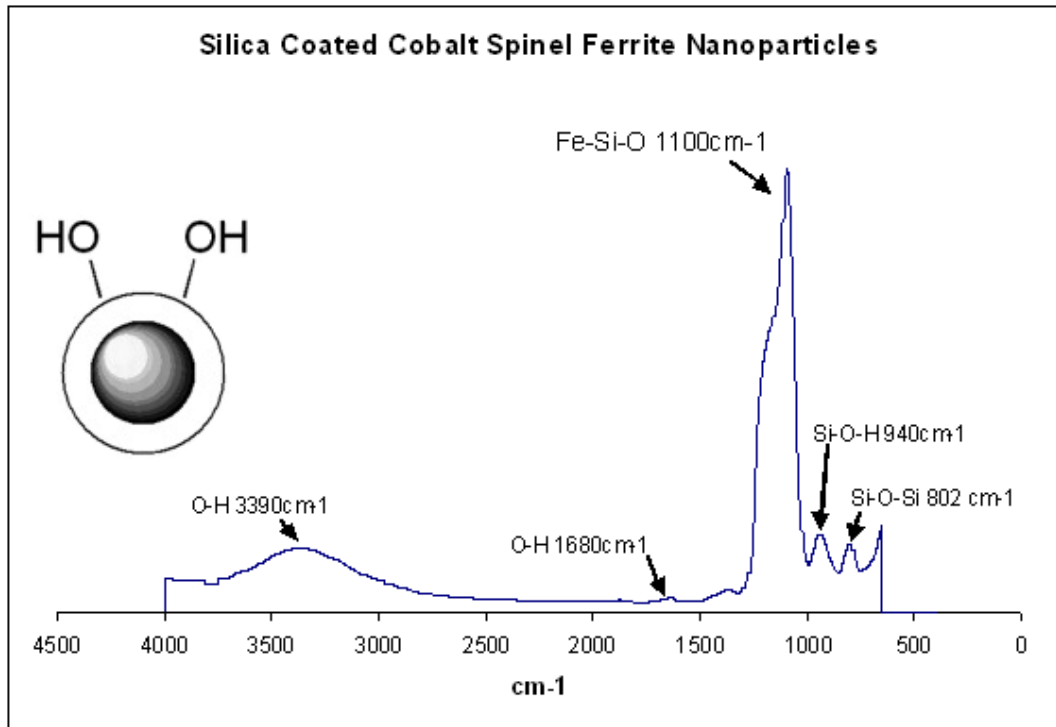
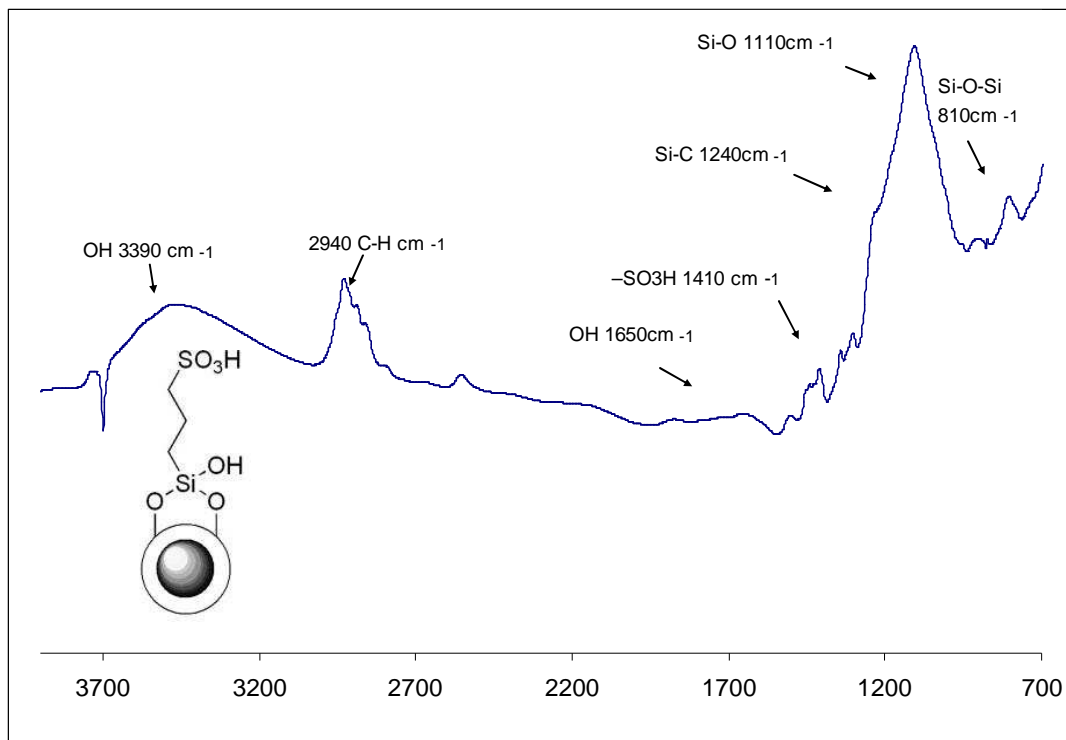
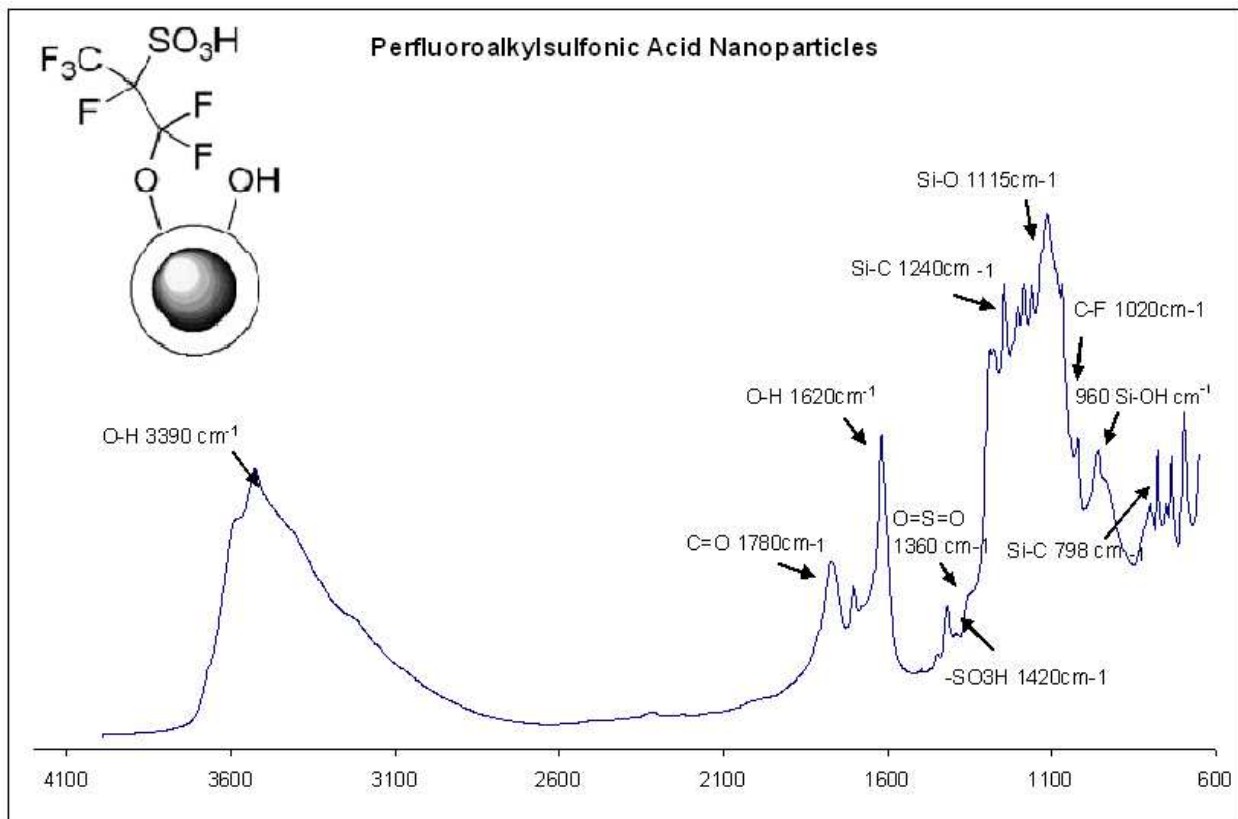


Figure 3-12 FTIR spectra of silica-coated nanoparticles



**Figure 3-13 FTIR spectra of alkyl-sulfonic acid nanoparticles**

Alvaro et al. (2005) identified the peak at 1420  $\text{cm}^{-1}$  as the peak assigned to the undissociated  $-\text{SO}_3\text{H}$  groups (Fig. 3-13 and 3-14). Suganuma et al. (2008) reported the vibration bands at 1040  $\text{cm}^{-1}$  for the stretching of the  $\text{SO}_3$  and 1377  $\text{cm}^{-1}$  for the  $\text{O}=\text{S}=\text{O}$  stretching in  $\text{SO}_3\text{H}$  group. Although the peaks between 1100 and 1200  $\text{cm}^{-1}$  are assigned to the C-F bond, it is overlapped by the peak of the Si-O bond (Kim 2003; Scaranto 2008). Biloiu et al. (2004) reported the bands between 1020 and 1220  $\text{cm}^{-1}$  as the peaks associated to the CF, CF<sub>2</sub>, and CF<sub>3</sub>, respectively.



**Figure 3-14 FTIR spectra of perfluoroalkyl-sulfonic-acid nanoparticles**

### **3.4.3 Acid Loading**

The acid sites were quantified through ion exchange capacity titrations. Sodium chloride and tetramethylammonium salts were used to draw out the hydrogen ions from the nanoparticles to the solution. The solutions were titrated with a 0.01M NaOH solution until neutrality was reached. The values obtained were greater than the values previously reported in the literature (Table 3-1). Melero et al. (2002) found 1.2 mmol H<sup>+</sup>/g SiO<sub>2</sub> for alkyl-sulfonic acid bound to mesoporous silica, and Gill et al. 2007 reported 0.47 and 0.78 mmol/g for AS-SiMNPs and PFS-SiMNPs, respectively.

**Table 3-1 Acid Capacity Titration**

	Acid capacity titration (mmolH <sup>+</sup> /g)		Initial pH after ion exchange (0.05 g catalyst)	Literature values (mmol/g)
	Na+	TMA+		
PFS-SiMNPs	1.92	1.82	2.28	0.47 <sup>a</sup>
AS-SiMNPs	0.99	0.93	2.95	0.78 <sup>a</sup>
CA-SiMNPs	0.41	0.21	4.16	-

Data from <sup>a</sup>( Gill et al. 2007)

### 3.5 Conclusions

TEM images of the cobalt spinel ferrite indicate that monodisperse nanoparticles were obtained with particle sizes less than 10nm, with clear interface between the magnetic core and the silica shell. TEM images of the cobalt spinel ferrite nanoparticles after the coating and acid functionalization indicate that coating and acid functionalization did not significantly affect the size and dispersion properties of the particles. The peaks at 802, 940, 1100, and 1680 cm<sup>-1</sup> on the FTIR spectra of the silica-coated magnetic nanoparticles are evidence of covalent bonding between the magnetic core and the silica layer. The peaks at 1110, 1020, 1240, 1650, 2940, and 3390 cm<sup>-1</sup> of the FTIR spectra of the alkyl-sulfonic acid-functionalized silica-coated magnetic nanoparticles are evidence of covalent bonding between the silica layer and the alkyl-sulfonic acid. The peaks at 798, 960, 1020, 1115, 1250, 1360, and 1620 cm<sup>-1</sup> on the FTIR spectra of the perfluoroalkyl-sulfonic acid-functionalized silica-coated magnetic nanoparticles are evidence of covalent bonding between the silica layer and the perfluoroalkyl-sulfonic acid.

Titration capacity of the synthesized acid-functionalized nanoparticles was higher than the values reported in the literature. However, to effectively catalyze the hydrolysis of  $\beta$ -glycosidic bonds, nanoparticles with higher acid strength are preferred. No clear relationship was found between the yield of glucan solubilized and the pH values, but the catalytic activity reduced to almost zero at the pH values around 7. High hydronium

ion concentrations facilitate the cellulose conversion but are not a determinant factor. The acidity strength of the  $\text{H}_3\text{O}^+$  ions decreased when solvated with water molecules; for that reason, it is believed that the sulfonic group, which should remain attached to nanoparticle, provides higher acidity than the hydronium ions in the solution. Stability and strength of the acid groups of the functionalized nanoparticles are necessary features for this particular application.

# **CHAPTER 4 - Biomass Pretreatment Using Acid-Functionalized Magnetic Nanoparticles**

## **4.1 Introduction**

The increasing energy demand and the decreasing oil availability have stimulated the research on new sources of energy. The more strict environmental regulations restrain replacement of energy sources to those that are renewable. Ethanol from fermentative processes is now considered an alternative for transportation fuel. Brazil is a remarkable example of production of fuel ethanol from sugar cane (Rothkopf 2007). Besides its technological capability and national policies, this South American country has an advantageous geographic position and land availability for sugar cane production that makes its fuel ethanol industry economically feasible (Sperling and Gordon 2009). Sugar cane has the advantage over other crops in that its carbohydrate components can be fermented without previous treatment.

Conversely, grains such as corn and sorghum have their carbohydrates in the form of starch. This sugar polymer needs to be cooked in order to obtain sugar monomers (glucose) for its subsequent conversion to ethanol. The hydrolysis of starch to obtain glucose is a relatively easy process and the fermentation to alcohol can be made simultaneously. However, utilization of cereal crops for fuel purposes has initiated a lot of debate. A dramatic increase in ethanol production using the current grain-starch-based technology will put stress on grain supplies which compete for limited agricultural land also needed for food and feed production.

Biomass is a potential source of energy to supply much of our transportation fuel needs. The United States currently consumes more than 140 billion gallons of transportation fuels annually. Conversion of cellulosic biomass such as agricultural residues to biofuels offers major economic, environmental, and strategic benefits. DOE and USDA projected that U.S. biomass resources could provide approximately 1.3 billion dry tons of feedstock (998 million dry tons from agricultural residues) for biofuels, which would meet at least 40% of the annual U.S. fuel demand for transportation

(Perlack 2005). In fact, biomass already supplies 40-50% of the energy demand in many developing countries (Hall and Moss 1983; Demirbas 2001).

Fermentable fractions of lignocellulosic biomass include cellulose and hemicellulose. Cellulose is highly crystalline, water insoluble, and highly resistant to depolymerization. Utilization of cellulosic sugars faces significant technical challenges. Cellulose is a linear polymer of D-glucose units linked by ( $\beta$ -1, 4-linked) glucose. Orientation of the linkages and additional hydrogen bonding make the polymer rigid and difficult to break (Van Hooijdonk 2005). Hemicelluloses are heterogeneous polymers of pentoses such as xylose and arabinose, hexoses such as mannose, glucose, and galactose, and sugar acids. They are generally cataloged according to the main sugar residue in the backbone (e.g., xylans, mannans, and glucans), with xylans and mannans being the most common (Wyman 2005). Unlike cellulose, hemicelluloses are not chemically homogeneous. Hemicellulose, because of its branched, amorphous nature, is relatively easy to hydrolyze (Van Hooijdonk 2005). Lignin is a long-chain, heterogeneous polymer composed largely of phenyl propane units most commonly linked by ether bonds (Saha 1997). Lignin restricts hydrolysis by shielding cellulose surfaces or by adsorbing and inactivating enzymes. It is understood that the close union between lignin and cellulose prevents swelling of the fibers, thereby affecting enzyme accessibility to the cellulose.

The polymers of glucose are joined by glycosidic bonds. These polymers have been hydrolyzed with acid or basic solutions, with steam or hot water (Herrera 2004; Jacobsen 2002; Liu 2005). High sugar yields have been reached with acid hydrolysis treatments using sulfuric acid (Corredor 2008). However, even low concentrations of sulfuric acid can cause degradation of glucose to hydroxymethylfurfural and other undesirable compounds (Mosier 2002). Use of sulfuric acid also requires a greater investment because the equipment wears out faster, and the waste materials obtained from the hydrolysis have to be separated and disposed.

Acid-supported materials have been successfully used for a diverse number of catalytic organic reactions. Nanoporous silicas with acid sites have effectively been used in liquid phase reactions (Alvaro 2005; Bootsma and Shanks 2007; Lien 2007). Kitano et al. (2009) used amorphous carbon-bearing,  $\text{HSO}_3$ ,  $\text{COOH}$ , and  $\text{OH}$  groups to

hydrolyze short  $\beta$ -1,4 glucans. The hydrolysis was carried out at 90°C with 0.0175 g of substrate/g catalyst, resulting in up to 15% of sugar yield. When they increased the content to 1.2 g cellobiose/g catalyst at the same temperature, up to 80% glucose yields was obtained after 24h of hydrolysis.

Monodisperse nanoparticles have an advantage over amorphous solids; monodisperse nanoparticles can behave like a fluid solution. If the nanoparticles happen to have magnetic behavior, the particles can be recovered from solution by applying a magnetic field. Nanoparticles, as well as mesoporous materials, can be functionalized; their chemical properties can be tuned conveniently. Therefore, using acid magnetic functionalized nanoparticles would potentially provide the benefits of the acid solutions with the advantage that they can be recovered and reused. The objective of this research aims to evaluate the hydrolysis performance of magnetic nanoparticles functionalized with three different acid functions: citric, alkyl-sulfonic, and perfluoroalkyl-sulfonic acids. Wheat straw, wood fiber and cellobiose were used as substrates to evaluate the catalytic activity of these nanoparticles.

## **4.2 Materials and Methods**

### **4.2.1 Hydrolysis of Biomass**

The hydrolysis performance of magnetic nanoparticles with two different acid functions including alkyl-sulfonic acid (AS), perfluoroalkyl-sulfonic acid (PFS) was evaluated for wheat straw, wood fiber, and cellobiose. The compositional analysis on a dry basis for both wheat straw and wood fiber is shown in Table 4-1. For hydrolysis, the two sulfonic acid-functionalized nanoparticles were tested at loading rates from 1.3-2.4% with biomass loadings from 2 to 4 % (w/w). The hydrolysis was carried out in pressure bottles for 24h at 80°C. All bottles were sealed to avoid mass loss. Hydrothermolysis controls were run for all experiments. An aliquot from the liquid fraction was neutralized with  $\text{CaCO}_3$ , filtered, and analyzed by HPLC using a RCM-Ca monosaccharide column (300 x 7.8mm; Bio-Rad, Richmond, CA.) and refractive index detector. Samples were run at 85°C, and eluted at 0.6ml/min with  $\text{H}_2\text{O}$ . Hemicellulose

yield was counted as the amount of D(+)glucose, D(+)xylose, D(+)mannose and D(+)arabinose derived from hemicelluloses. The concentration of D-cellobiose couldn't always be read by interference of other compounds present in the liquid fraction.

**Table 4-1 Biomass compositional analysis**

Biomass feedstock constituents	Wheat straw	Wood fiber
95% ethanol extractives	13.0	20.6
Ash (%)	10.3	0.6
Acid Soluble Lignin (%)	2.3	1.1
Acid-Insoluble Lignin (%)	15.9	26.3
Total Lignin (%)	18.2	27.4
Xylan (%)	21.7	14.5
Glucan (%)	37.6	36.1
Mannan (%)	0.3	1.2

#### ***4.2.2 Total Carbohydrates Analysis:***

It has been found that hydrolysis of cellulose with solid supported acid gave low monosaccharide yields; most of the sugars were converted to long chain sugars (Suganuma 2008). In order to count the amount of sugars that were solubilized, the supernatant was further hydrolyzed to convert oligosaccharides into sugars with lower molecular weight. The hydrolysis was done following the NREL LAP procedure TP-510-42618 (Sluiter 2008). Seventy-two percent sulfuric acid (w/w) was used to bring the acid concentration to 4% (w/w). The sealed samples were autoclaved at 121°C for 1h. The neutralized samples were analyzed by HPLC.

#### ***4.2.3 Enzymatic Hydrolysis***

In order to evaluate the possibility of using acid-functionalized nanoparticles in combination with enzymes, the digestibility test was effectuated upon some of the

pretreated samples Selig et al. (2008). The biomass was separated from the catalyst and rinsed with abundant water. Accellerase™ 1000 from Genencor, Inc. was used for enzymatic hydrolysis. The hydrolysis was carried out for 72h, after which the samples were placed in HPLC vials for subsequent analysis.

## **4.3 Results and Discussion**

### ***4.3.1 Monosaccharides Yield***

Very few monosaccharides were obtained from wheat straw and wood fiber after treatment with acid-functionalized nanoparticles (Figures 4.1-4.2). The sugar yield as hemicellulose was obtained from the liquid fraction. Hemicellulose yields as high as 31 % were obtained from wheat straw (Figure 4-1); meanwhile, yields up to 10% were obtained from wood fiber (Figure 4-2). Wood fiber is a more recalcitrant material compare to herbaceous crops such as wheat straw. This result is in agreement with Suganuma et al (2008). They used acid-functionalized amorphous carbon to hydrolyzed cellulose and reported monomers yield of only 4%; most of the sugars obtained were in oligomeric form. Although cellobiose was obtained from the biomass samples in few amounts, its production should be avoided due to that cellobiose is inhibitory of cellulases (Lopez santin 1985; Alonso 2001) and it can't be fermented by common yeast strains.

Because cellobiose, the smallest oligosaccharide, has been used as the model material for cellulose degradation to glucose in some studies (Furukawa 2002; Bootsma 2007), performance of the catalysts upon cellobiose was also measured. Unfortunately, the sugar was poorly affected by the catalysts; from 1100 mg of available glucose in the initial solution, only 6.1% was converted into the glucose monomer.

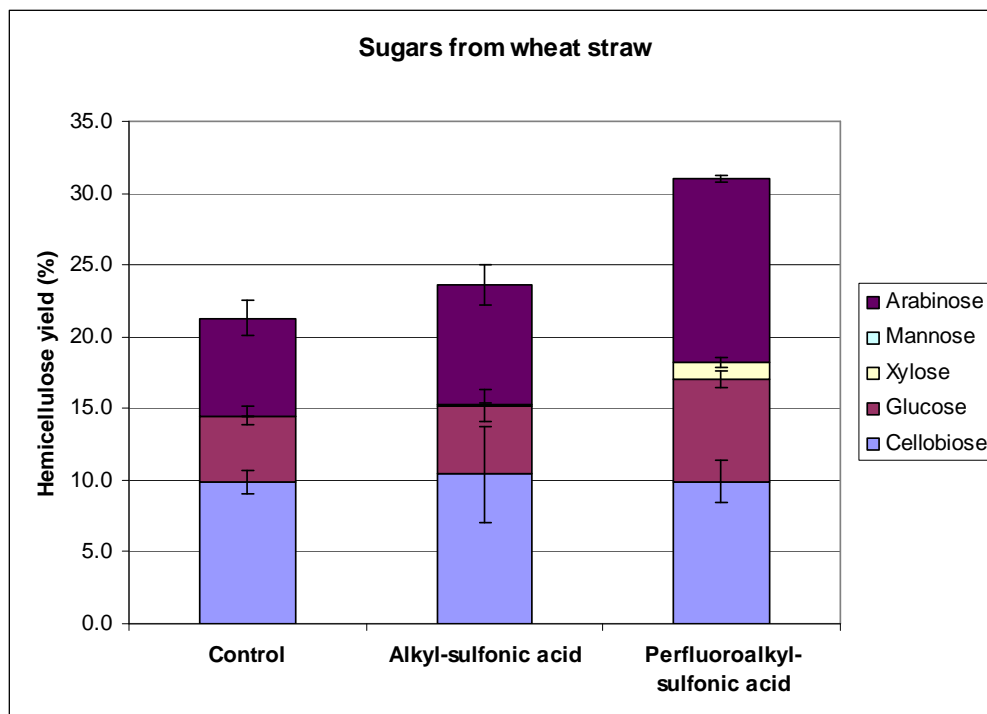


**Figure 4-1 Monomer sugars and cellobiose yields from wheat straw after pretreated with PFS and AS acid functionalized nanoparticles at 80°C for 24h**

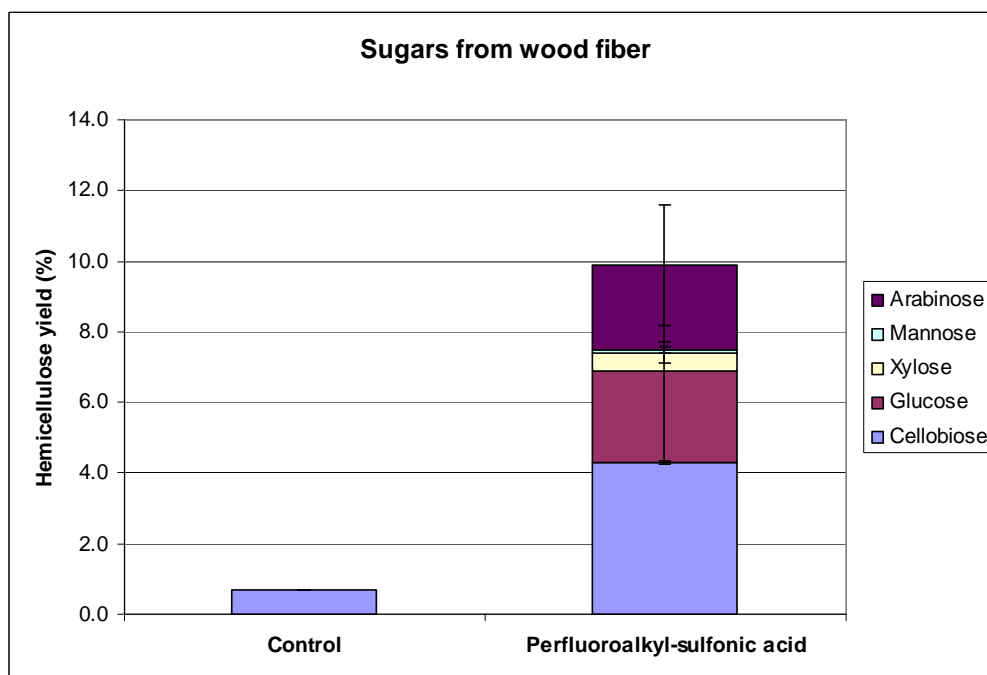


**Figure 4-2 Monomer sugars and cellobiose yields from wood fiber after pretreated with PFS acid functionalized nanoparticles at 80°C for 24h**

### 4.3.2 Total Sugars Yield

If the acid-functionalized nanoparticles are able to hydrolyze cellulose to the monomers, the next step in the process would be alcoholic fermentation of the solubilized sugars, and the enzymatic hydrolysis step could be eliminated. However, if the acid-functionalized nanoparticles only degrade hemicellulose to short chain polymers of glucose, xylose, mannose and arabinose, the acid-functionalized treatment has to be followed by an enzymatic hydrolysis. In this instance, lignin and hemicellulose removal is aimed and high glucose recovery is expected. As previously found (Mosier 2002), the solid acid catalysts degrade the polysaccharides into oligomeric forms rather than to monomers. In order to quantify the total amount of sugars obtained after the catalyst treatment, the supernatant was further hydrolyzed to split the solubilized long-chain sugars into monomers. The amount of solubilized sugars from wheat straw and wood fiber is shown in Figures 4-3 and 4-4 as hemicellulose yield.

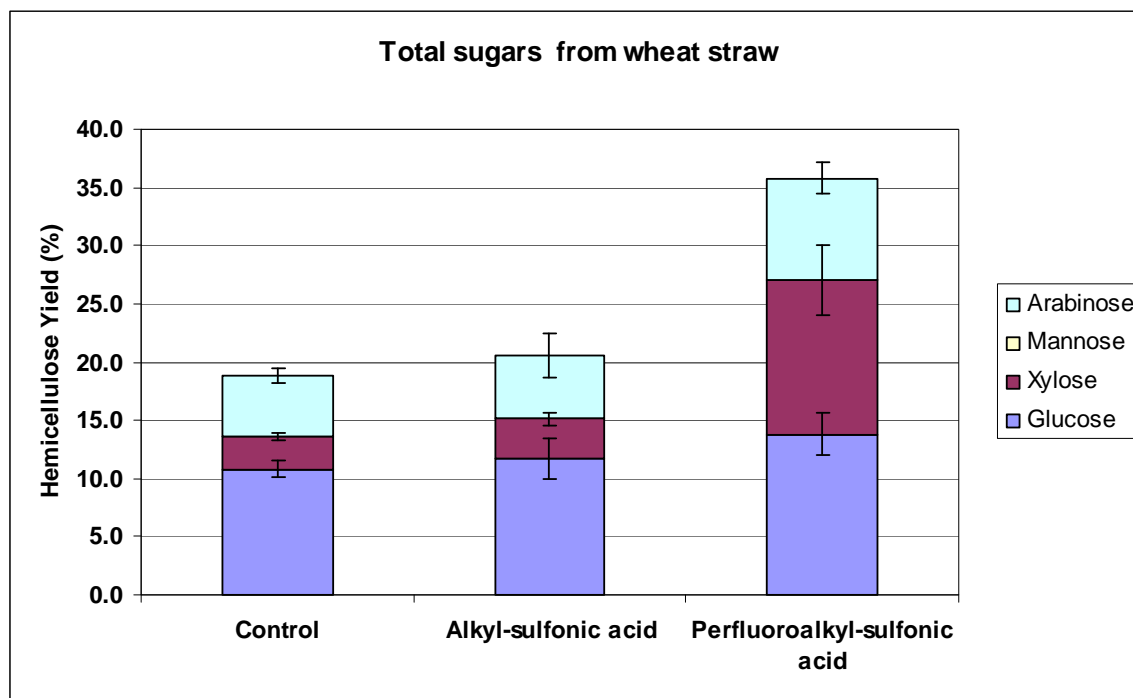
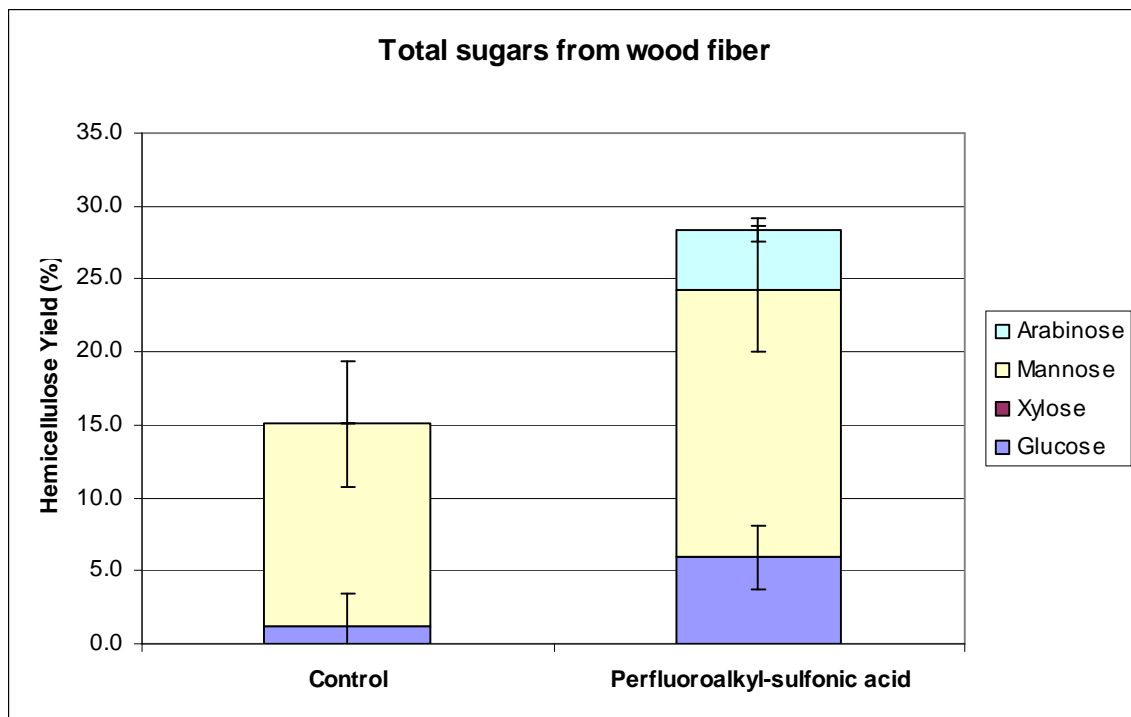


Figure 4-3 Total sugar yield from wheat straw after pretreated with PFS and AS acid functionalized nanoparticles at 80°C for 24h



**Figure 4-4 Total sugar yield from wood fiber after pretreated with PFS acid functionalized nanoparticles at 80°C for 24h**

The control for all the experiments is the treatment of the sample with the same conditions of the other samples, except that the control doesn't have a catalyst. In this instance, only the thermolysis is the driving force that causes the hydrolysis of sugars. We wanted to determine the hydrolysis ability of the catalyst eliminating the heating effect. Yields of total sugars obtained from wheat straw treated with alkyl-sulfonic acid functionalized nanoparticles were not significantly different from the control. The sugar yields from wheat straw treated with perfluoroalkyl-sulfonic acid nanoparticles were significantly higher than that from the control (p-value for this experiment was equal to 0.0016). On the other hand, the same catalyst also made a difference in the treatment of wood fiber; the hemicellulose yield increased from 15.1 to 28.4% when perfluoroalkyl-sulfonic acid-functionalized nanoparticles were used.

Wood fiber is a more recalcitrant material compared to herbaceous crops such as wheat straw. The yield of solubilized hemicellulose from wheat straw was higher than that from wood fiber. The original wheat straw and wood fiber samples were not

extractives free and some of the sugars accounted for could have been soluble sugars in the sample.

#### 4.3.4 Hydrolysis of extractives-free Wood Fiber and Wheat Straw

To avoid the effects of soluble sugars in the biomass on total sugar yield after treatment, wheat straw and wood fiber were subjected to both water and alcohol extraction. The samples were refluxed with water for 24h in a soxhlet apparatus and another 24h with 95% ethanol. After the extraction process, the wood fiber sample was dried at 103°C for 24h and the wheat straw sample at 45°C for 72h. For wheat straw extractives-free (Figure 4-5 and Figure 4-6) and wood fiber extractives-free (Figure 4-7 and Figure 4-8), the amount of sugars solubilized in the presence of perfluoroalkyl-sulfonic acid nanoparticles (PFS-SiMNPs) showed a significant increase of solubilized sugars with respect to the control (p-value was lower than 0.0001). Same result was observed for wood fiber extractives-free (p-value=0.0064).

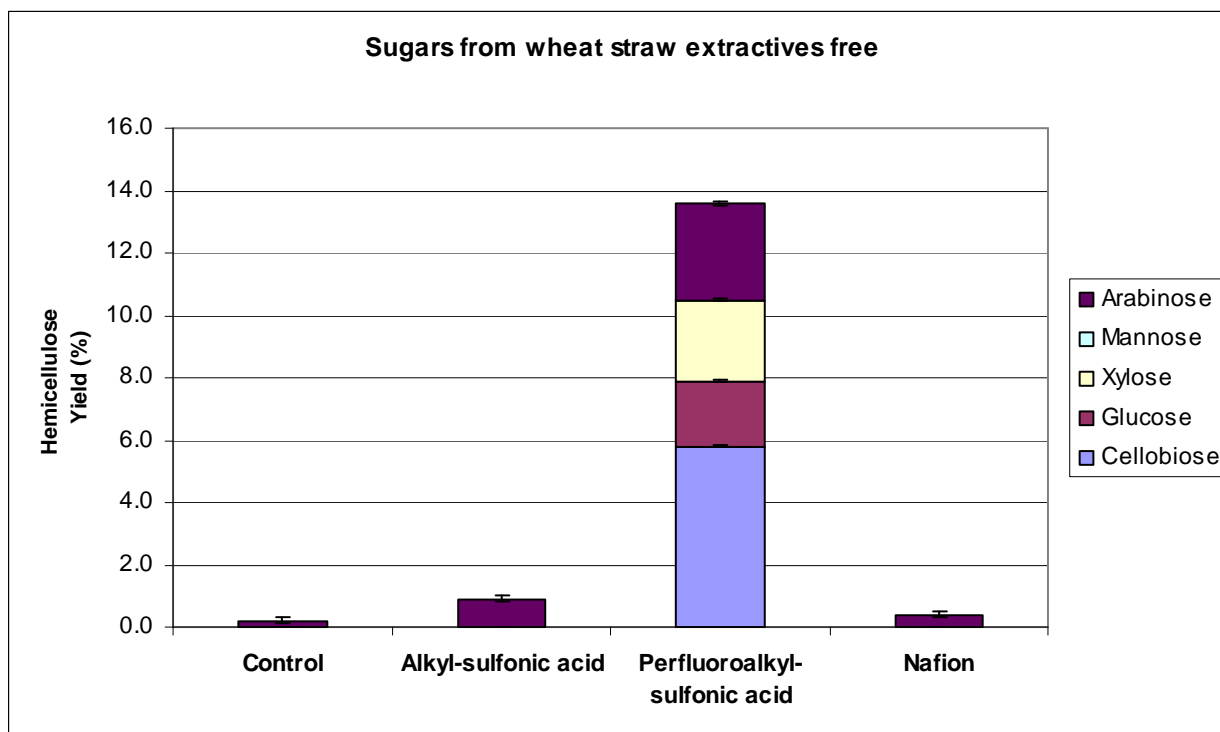
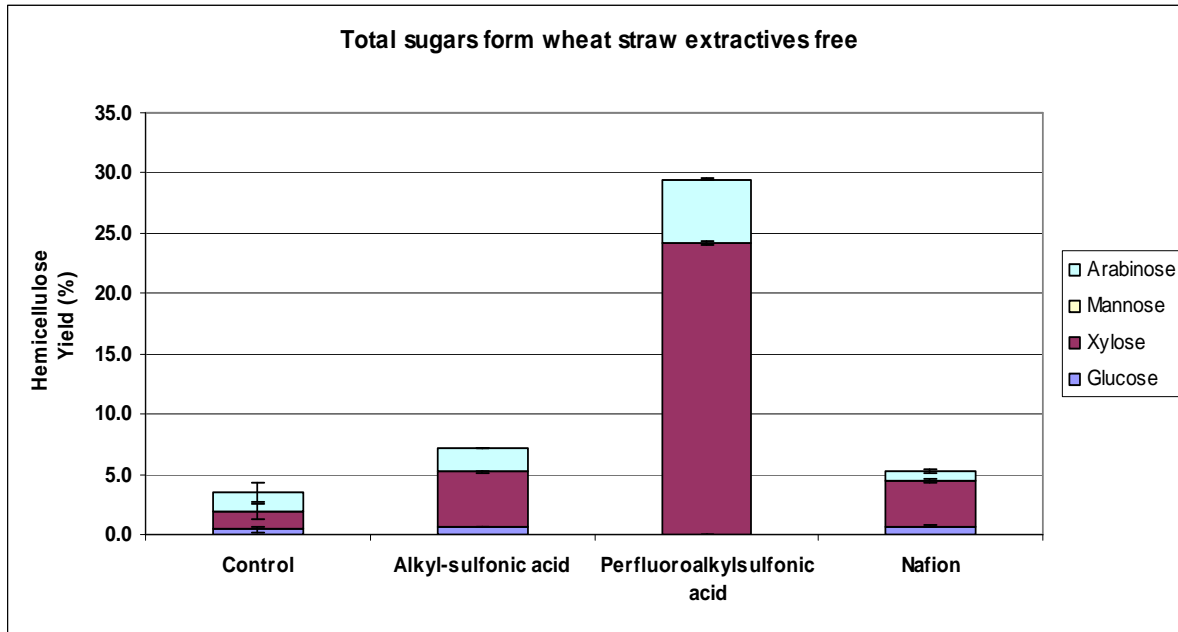
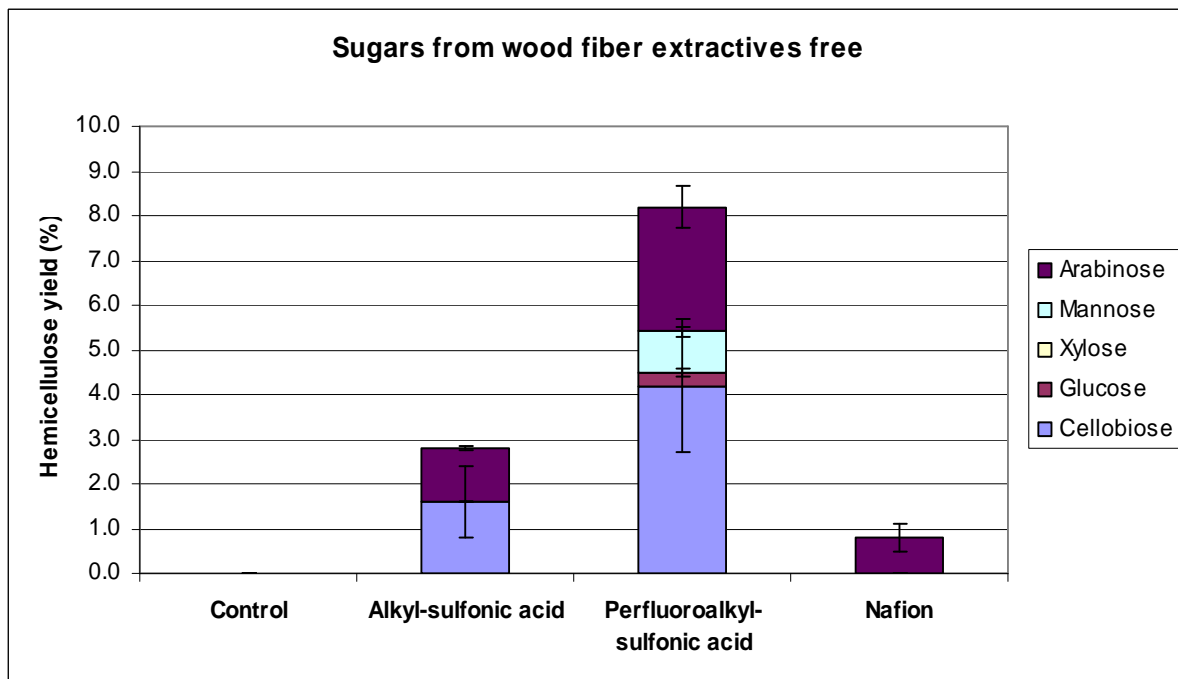


Figure 4-5 Monomer sugars yield and cellobiose from wheat straw extractives free after pretreated with PFS acid functionalized nanoparticles at 80°C for 24h



**Figure 4-6 Total sugar yield from wheat straw extractives free after pretreated with PFS acid functionalized nanoparticles at 80°C for 2 h**



**Figure 4-7 Monomer sugars yield and cellobiose from wood fiber extractives free after pretreated with PFS acid functionalized nanoparticles at 80°C for 24h**

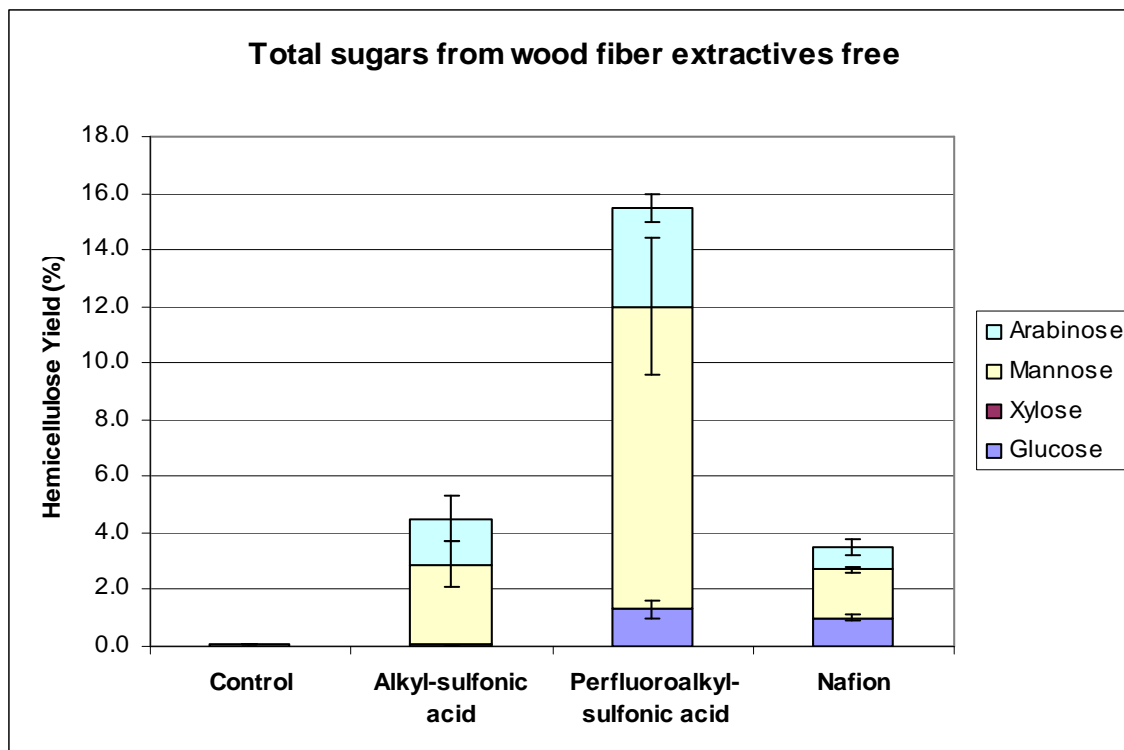


**Figure 4-8 Total sugar yield from wood fiber extractives free after pretreated with PFS acid functionalized nanoparticles at 80°C for 2 4h**

#### ***4.3.5 Enzymatic Hydrolysis***

The purpose of the pretreatment methods is the exposition of the cellulose to the active sites of the enzymes, rather than a complete solubilization of sugars. Ideally, the acid-functionalized nanoparticles would do the entire job, pretreatment and enzymatic hydrolysis, all at once. Because at 80°C the catalyst was only able to degrade hemicelluloses, the combined performance of both acid nanoparticles treatment and enzymatic hydrolysis on sugar yields was considered.

Results of the digestibility test are shown in Table 4-2. Treatment of wheat straw with PFS and AS acid-functionalized nanoparticles could have caused inhibition of the enzymatic hydrolysis; the digestibility of the samples that were pretreated with the catalysts decreased with respect to the sample that just had gone the thermolysis treatment.

**Table 4-2 Digestibility of biomass after pretreatment with acid catalysts**

Biomass	Catalyst	Digestibility (%)
Wheat straw (as received)	PFS	<b>20.3</b>
	AS	<b>19.1</b>
	control	<b>37.8</b>
Wheat straw, extractives free	PFS	<b>26.7</b>
	AS	<b>16.0</b>
	control	<b>37.3</b>
Wood fiber, extractives free	PFS	<b>11.4</b>
	AS	<b>8.0</b>
	control	<b>8.5</b>

\*PFS=perfluoroalkyl-sulfonic acid nanoparticles; AS=alkyl-sulfonic acid nanoparticles.

#### **4.3.6 Effect of the pH**

pH values of the reaction solutions at the end of the hydrolysis at 80°C for the control, PFS-SiMNPs, Nafion, and AS-SiMNPns solutions are shown in Table 4-3. Several authors have effectively used dilute sulfuric acid in the pretreatment of lignocellulosic materials (Mosier et al. 2005; Liu and Wyman 2004). The pH of dilute sulfuric acid solutions (e.g., 0.05 - 1% wt/wt) can be lower than 1.5 at the end of hydrolysis. To decrease the pH at these levels would require either utilizing higher load of the catalyst or increasing the number of acid sites per gram of catalyst. The neutralization effect of the biomass minerals also consumes some of the available acid sites (Hashimoto 1997); therefore, samples with higher ash content would require a larger catalyst load.

Even though low pH values usually give higher yields (Figure 4-9), a clear correlation between pH and sugar yield is not observed; other factors different than

hydronium ion concentration also affect the acid hydrolysis of biomass. Kitano et al. (2009) used solid acids to break  $\beta$ -1,4 glycosidic bonds and found that the presence of COOH and phenolic OH as surface functional groups help the hydrolytic activity of the sulfonic acid groups. According to these authors, COOH and phenolic OH groups help the absorption of  $\beta$ -1,4-glucan that is later hydrolyzed by SO<sub>3</sub>H groups. Therefore, in order to improve the catalytic activity of acid-functionalized nanoparticles, adding the attachment of sulfonic acids groups, and simultaneous functionalization with COOH and acidic OH is recommended.

**Table 4-3 pH of the solution at the end of pretreatment**

Biomass	Catalyst*	Total sugars yield (%)	pH
Wheat straw	PFS	<b>35.8</b>	<b>3.45</b>
	AS	<b>20.5</b>	<b>4.87</b>
	control	<b>18.8</b>	<b>5.07</b>
Wheat straw, extractives free	PFS	<b>29.5</b>	<b>1.86</b>
	AS	<b>7.1</b>	<b>2.53</b>
	Nafion SAC13	<b>5.3</b>	<b>3.56</b>
	control	<b>3.5</b>	<b>4.25</b>
Wood fiber	PFS	<b>28.4</b>	<b>2.60</b>
	control	<b>15.1</b>	<b>7.26</b>
Wood fiber, extractives free	PFS	<b>15.5</b>	<b>2.60</b>
	AS	<b>4.5</b>	<b>2.64</b>
	Nafion SAC13	<b>3.5</b>	<b>3.75</b>
	control	<b>0.1</b>	<b>7.05</b>

\*PFS=perfluoroalkyl-sulfonic acid nanoparticles and AS=alkyl-sulfonic acid nanoparticles.

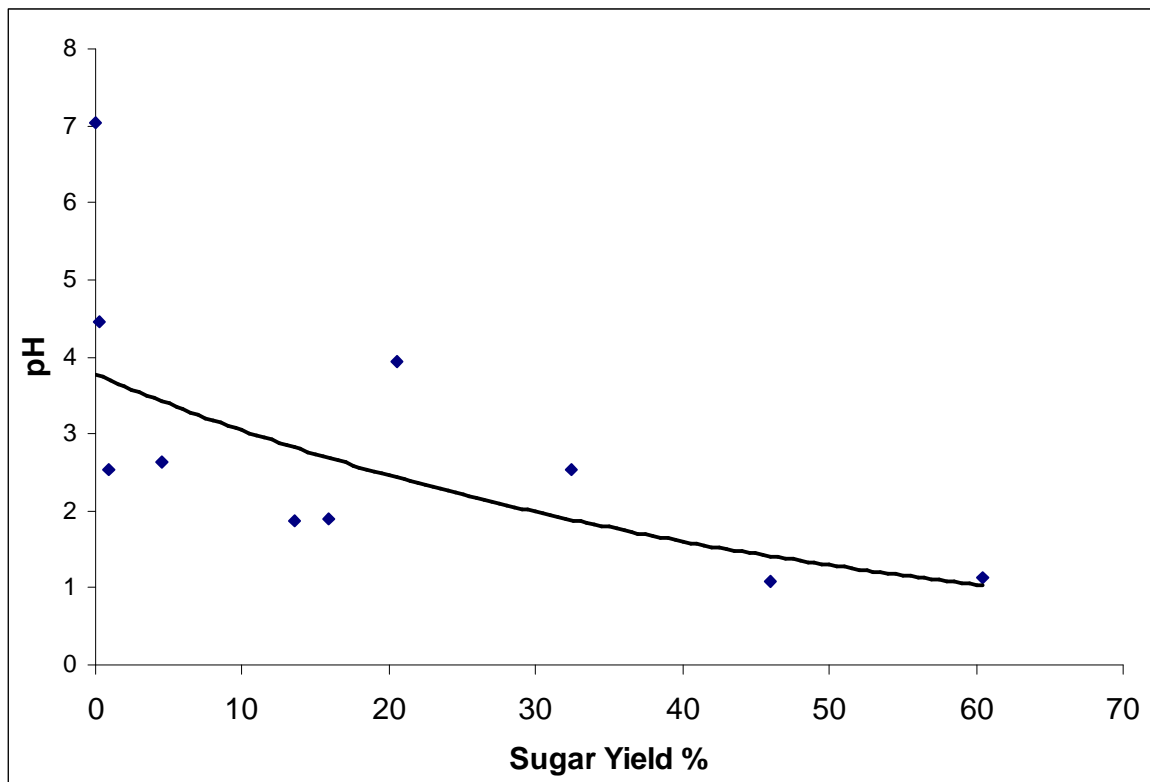


**Figure 4-9 pH vs sugar yield plot for wheat straw and wood fiber, extractives free**

#### **4.3.7 Performance of the Catalysts**

Nanoparticles functionalized with perfluoroalkyl-sulfonic acid showed the highest sugar yields with respect to the control. Moderate yields of hemicelluloses were obtained at 80°C when compared to the hydrolysis at 160°C (Zhao 2009). Fluoroalkyl-sulfonic acids belong to the superacids catalyst category. Numerous studies have reported use of fluoroalkyl-sulfonic acids supported on mesoporous silica (Sluiter et al. 2008). The high acid strength of these acids has been explained by the electron withdrawing properties of the Fluor atoms (Suganuma et al. 2008). The better capacity for breaking glycosidic bonds may be attributed to the higher amount of hydronium ions in the solution, as was evidenced by lower pH for the PFS-SiMNPs. Some authors have discussed possible mechanisms for the hydrolysis of the glycosidic bonds in more detail (Moldes et al. 2001).

Performance of nanoparticles functionalized with alkyl-sulfonic acid didn't show a significant improvement on hemicellulose yields. As previously reported (Lopezasantin et

al. 1985), the acid loading for this catalyst was relatively low. However, low catalytic activity could have been a consequence of the poor water affinity observed for this catalyst. These results agree with the findings of Van Rhijn et al. (1998) and Bootsma and Shanks (2007).

Gill et al. (2007) and Suganuma et al. (2008) reported that acid groups in the PFS nanoparticles were leached into the reaction solution. Catalytic activity for the deprotection reaction of benzaldehyde dimethylacetal was at room temperature was attributed to acid groups in the solution; the catalysis was considered as a homogeneous catalyst. Only if the reaction is helped out by the acid groups attached to the surface of the nanoparticles, is the catalysis considered as heterogeneous. Titration results after the hydrolysis of biomass at 80°C are shown in Table 4-4. The acid capacity was lost in the first run for both acid-functionalized nanoparticles. If the catalyst doesn't retain its acid groups, it couldn't be reused. These results suggest that the recyclability requirement is not filled by the catalysts.

**Table 4-4 Sulfonic acid loading before and after reaction**

	Titration loading (mmolH <sup>+</sup> /g)	Initial pH after ion exchange (0.05gcatalyst)	Titration loading after reaction (mmolH <sup>+</sup> /g)
PFS-SiMNPs	1.92	2.14	0.20
AS-SiMNPs	0.99	2.95	0.17

\*PFS=perfluoroalkyl-sulfonic acid nanoparticles; AS=alkyl-sulfonic acid nanoparticles.

#### **4.3.8 Effect of Temperature**

Because of thermodynamic barriers, some scientists affirm that if either the acid concentration or the temperature is too low, the other variable has to be increased to compensate for the change (Sun 2009). In our instance, both acid concentration and temperature were low, and still some sugars were solubilized.

According to Bootsma et al. (2007) at the pH ranges we worked with, 24h is enough to degrade cellobiose to glucose completely when the temperature is around 145°C. Because at low temperatures the hydrolysis rate constant of the reaction is very small, in order to convert cellobiose to glucose we will need either longer times, or higher temperatures, or greater hydronium ion concentrations. Nonetheless, the acid-functionalized nanoparticles would still be useful if the cellulose recovery is high. This means that the glucan yield should be low; meanwhile, the lignin and xylan removal are expected to be high. The cellulose shouldn't be solubilized but remain in the solid that would be subjected later to enzymatic hydrolysis. Some preliminary experiments at a higher temperature were executed. As shown in Table 4-5, using PFS nanoparticles at 120°C for 2h gave about the higher hemicellulose yield and about same digestibility values as the hydrolysis reaction at 80°C for 24h.

**Table 4-5 Hemicellulose yield from wood fiber hydrolysis at 120°C for 2h**

catalyst	Sugar yield (%)	pH	Digestibility (%)
none	<b>0.0</b>	<b>5.78</b>	<b>9.7</b>
Nafion SAC13	<b>5.4</b>	<b>4.12</b>	<b>9.5</b>
PFS	<b>47.0</b>	<b>2.63</b>	<b>9.3</b>

\*PFS=perfluoroalkyl-sulfonic acid nanoparticles.

#### **4.4 Conclusions**

Hydrolysis of wheat straw with acid-functionalized nanoparticles at 80°C for 24h didn't release a significant amount of monosaccharides relative to hydrothermolysis. However, analysis of sugars in the liquid fraction of the hydrolysis revealed a significant amount of oligosaccharides compare to the hydrothermolysis. The acid-functionalized nanoparticles broke down the nonsoluble polysaccharides to oligomeric forms. The hydrolysis of wood fiber resulted in a better effectiveness of these catalysts to degrade

hemicellulose polymers. The alkyl-sulfonic and perfluoroalkyl-sulfonic acid groups from the nanoparticles converted part of the hemicellulose polymer to soluble oligosaccharides. The alkyl-sulfonic acid-functionalized nanoparticles showed a low effectiveness in the catalysis of the hemicellulose degradation. The low water affinity of these nanoparticles restrains their use to non-polar mediums. On the other hand, the perfluoroalkyl-sulfonic acid nanoparticles easily leaked their acid moieties; the recyclability requirement to be used in the biomass conversion was not fulfilled.

# CHAPTER 5 - Conclusions and Recommendations for Further Research

## 5.1 Conclusions

Acid-functionalized nanoparticles were synthesized for pretreatment and hydrolysis of lignocellulosic biomass to increase the conversion efficiency of biomass at mild conditions. TEM images and FTIR were used to characterize the properties of acid-functionalized nanoparticles in terms of nanoparticle size and presence of sulfonic acid functional groups; pH and ion exchange titrations were used as indicators of the acid sites present. Wheat straw, wood fiber and cellobiose were used as raw materials to evaluate the hydrolysis performance of acid-functionalized nanoparticles.

1. TEM images of cobalt spinel ferrite indicate that monodisperse nanoparticles were obtained with particle sizes less than 10 nm and a clear interface between the magnetic core and the silica shell. TEM images of cobalt spinel ferrite nanoparticles after the coating and acid functionalization indicated that coating and acid functionalization did not significantly affect size and dispersion properties of the particles.

2. Peaks at 802, 940, 1100, and 1680  $\text{cm}^{-1}$  on the FTIR spectra of the silica-coated magnetic nanoparticles are evidence of covalent bonding between the magnetic core and the silica layer. Peaks at 1110, 1020, 1240, 1650, 2940, and 3390  $\text{cm}^{-1}$  of the FTIR spectra of the alkyl-sulfonic acid-functionalized silica-coated magnetic nanoparticles are evidence of covalent bonding between the silica layer and the alkyl-sulfonic acid. Peaks at 798, 960, 1020, 1115, 1250, 1360, and 1620  $\text{cm}^{-1}$  on the FTIR spectra of the perfluoroalkyl-sulfonic acid-functionalized silica-coated magnetic nanoparticles are evidence of covalent bonding between the silica layer and the perfluoroalkyl-sulfonic acid.

3. Titration capacity of the synthesized acid-functionalized nanoparticles was higher than the values reported in the literature. However, to effectively catalyze the hydrolysis

of  $\beta$ -glycosidic bonds, nanoparticles with higher acid strength are preferred. No clear relationship was found between the yield of glucan solubilized and the pH values, but catalytic activity reduced to almost zero at pH values around 7. High hydronium ion concentrations facilitate cellulose conversion but are not a determinant factor. Acidity strength of the  $\text{H}_3\text{O}^+$  ions decreased when solvated with water molecules; for that reason, it is believed that the sulfonic group, which should remain attached to nanoparticle, provides higher acidity than the hydronium ions in the solution. Stability and strength of the acid groups of the functionalized nanoparticles are necessary features for this particular application.

4. Hydrolysis of wheat straw with acid-functionalized nanoparticles at 80°C for 24h didn't release a significant amount of monosaccharides relative to hydrothermolysis. However, the analysis of sugars in the liquid fraction of the hydrolysis revealed a significant amount of oligosaccharides compared to the hydrothermolysis. The acid-functionalized nanoparticles broke down the nonsoluble polysaccharides to oligomeric forms. Hydrolysis of wood fiber resulted in a better effectiveness of these catalysts to degrade cellulose polymers. Alkyl-sulfonic and perfluoroalkyl-sulfonic acid-functionalized nanoparticles converted hemicelluloses to the short oligosaccharides. The alkyl-sulfonic acid-functionalized nanoparticles showed a low effectiveness in the catalysis of the hemicellulose degradation. The low water affinity of these nanoparticles restrains their use in non-polar mediums. On the other hand, the perfluoroalkyl-sulfonic acid nanoparticles easily leak their acid moieties; thus, the recyclability requirement to be used in the biomass conversion is not fulfilled.

## **5.2 Recommendations**

To continue further research in the catalytic activity of perfluoroalkylsulfonic acid nanoparticles, it is necessary to determine whether or not the catalytic activity of PFS nanoparticles is due to leached acid groups. In this case, the catalyst can't be considered as a heterogeneous catalyst. More rigorous analysis of the liquid phase is necessary to evaluate possible leaching of acid groups from the nanoparticles surface into the solution. Catalytic activity from acid moieties in the solution must be

differentiated from the hydrolysis caused by the acid groups attached to the surface of the nanoparticles.

Acid-functionalized nanoparticles with strong acid acidities, good water dispersion, and thermal stability are required to demonstrate their ability to break down glycosidic bonds. To improve the affinity of the nanoparticles with the biomass chemical components, besides the attachment of sulfonic acids groups, simultaneous functionalization with COOH and acidic OH is suggested.

Advanced technologies such as DSC and TGA analysis can be made to evaluate thermal stability and water affinity of the catalysts. Recyclability is an advantage of heterogeneous catalysts; to meet this condition, the catalysts should retain their acidity after being used for the hydrolysis of biomass. If the catalyst undergoes changes during the reaction, it can't be reused.

To allow recoverability, the catalyst doesn't have to be magnetic necessarily; a difference in density could be enough for separation of biomass and catalyst. Any metal core nanoparticles could eventually work because their density would be higher than the density of the biomass.

Pretreatment of biomass can also be handled with basic chemical agents. Commercial nanoparticles functionalized with amine groups are currently available. Utilization of commercial nanoparticles would save time in characterization. Better understanding of the mechanism of hydrolysis can be realized when more information about the physicochemical properties of the nanoparticles is known. Percentages of sulfur, molecular weight, surface area and thermal properties are valuable data.

Lignin and hemicellulose removal can be determined; solubilization of these components is, among others, one of the current goals of biomass pretreatment. The exposition of cellulose to the enzyme action could be favored by removal of lignin and hemicellulose using recyclable solid acids. Elimination of lignin and hemicellulose

polymers without solubilization of cellulose would also allow high sugar recoveries; therefore, more sugar would be available for enzymatic hydrolysis. Further studies of the effects that pretreatment with functionalized nanoparticles can make over enzymatic hydrolysis are recommended.

Common pretreatment methods use temperatures higher than 120°C; meanwhile, this study used only 80°C. To make a better comparison between current methods and the proposed method of pretreatment, higher temperatures should be used during the biomass pretreatment.

## References

- Adebiyi, F., J. Sonibare, O. Okelana and E. Obanijesu. 2009. Air-borne SO<sub>2</sub> pollution monitoring in the upstream petroleum operation areas of Niger-Delta, Nigeria. *Energy sources, part A: recovery, utilization, and environmental effects* 31(3): 223.
- Agrawal, M. and A. Singh. 2008. Acid rain and its ecological consequences. *Journal of Environmental Biology* 29(1): 15.
- Albright, L. 1990. H<sub>2</sub>SO<sub>4</sub>, HF Processes Compared, and New Technologies Revealed. *Oil Gas Journal* 88(48): 70.
- Allred, C. S., D. Arnold, T. J. Barrett, A. Beehler, A. Bement, G. Buchanan, T. C. Dorr, G. Gray, S. Hays, A. Karsner, R. Orbach, P. Swagel and J. Turner. 2008. National Biofuels Action Plan.
- Alvaro, M. 2005. "Nafion"-functionalized mesoporous MCM-41 silica shows high activity and selectivity for carboxylic acid esterification and Friedel-Crafts acylation reactions. *Journal of Catalysis* 231(1): 48.
- Alvaro, M., A. Corma, D. Das, V. Fornes and H. Garcia. 2005. "Nafion"-functionalized mesoporous MCM-41 silica shows high activity and selectivity for carboxylic acid esterification and Friedel-Crafts acylation reactions. *Journal of Catalysis* 231(1): 48.
- Averback, R., W. Brown, L. Brus, W. Goddard, A. Kaldor and R. Andres. 1989. Research Opportunities On Clusters And Cluster-Assembled Materials - A Department of Energy, Council on Materials Science Panel Report. *Journal of Materials Research* 4(3): 704.
- Bals, B., B. Dale and V. Balan. 2006. Enzymatic hydrolysis of distiller's dry grain and solubles (DDGS) using ammonia fiber expansion pretreatment. *Energy Fuels* 20(6): 2732-2736.

Biloiu, C., I. A. Biloiu, Y. Sakai, Y. Suda and A. Ohta. 2004. Amorphous fluorocarbon polymer (a-C : F) films obtained by plasma enhanced chemical vapor deposition from perfluoro-octane (C<sub>8</sub>F<sub>18</sub>) vapor I: Deposition, morphology, structural and chemical properties. *Journal of Vacuum Science Technology. A. Vacuum, surfaces, and films* 22(1): 13.

Bobleter, O. 1994. Hydrothermal degradation of polymers derived from plants. *Progress in Polymer Science* 19(5): 797.

Bootsma, J. A. and B. H. Shanks. 2007. Cellobiose hydrolysis using organic-inorganic hybrid mesoporous silica catalysts. *Applied Catalysis A-General* 327(1): 44-51.

Breslow, R. 1995. Biomimetic chemistry and artificial enzymes - catalysis by design. *Accounts of Chemical Research* 28(3): 146-153.

Calero-DdelC, V. L. and C. Rinaldi. 2007. Synthesis and magnetic characterization of cobalt-substituted ferrite (Co<sub>x</sub>Fe<sub>3-x</sub>O<sub>4</sub>) nanoparticles. *Journal of Magnetism and Magnetic Materials* 314(1): 60.

Cejpek, K., J. Velisek and O. Novotny. 2008. Formation of carboxylic acids during degradation of monosaccharides. *Czech Journal of Food Science* 26(2): 117.

Chafin, S., K. Pennybaker, D. Fahey, B. Subramaniam and K. Gong. 2008. Economic and environmental impact analyses of solid acid catalyzed isoparaffin/olefin alkylation in supercritical carbon dioxide. *Industrial Engineering Chemistry Research* 47(23): 9072.

Chen, Q. and Z. J. Zhang. 1998. Size-dependent superparamagnetic properties of MgFe<sub>2</sub>O<sub>4</sub> spinel ferrite nanocrystallites. *Applied Physics Letters* 73(21): 3156.

Corma, A., D. Das, V. Fornes, H. Garcia and M. Alvaro. 2004. Single-step preparation and catalytic activity of mesoporous MCM-41 and SBA-15 silicas functionalized with perfluoroalkylsulfonic acid groups analogous to Nafion (R). *Chemical Communications*(8): 956.

- Corma, A. and H. Garcia. 2006. Silica-bound homogeneous catalysts as recoverable and reusable catalysts in organic synthesis. *Adv.Synth.Catal.* 348(12+13): 1391-1412.
- Corredor, D. Y., X. S. Sun, J. M. Salazar, K. L. Hohn and D. Wang. 2008. Enzymatic hydrolysis of soybean hulls using dilute acid and modified steam-explosion pretreatments. *Journal of Biobased Materials and Bioenergy* 2(1): 43.
- Dale, B. and M. Lau. 2009. Cellulosic ethanol production from AFEX-treated corn stover using *Saccharomyces cerevisiae* 424A(LNH-ST). *Proceedings of the National Academy of Sciences of the United States of America* 106(5): 1368.
- Datar, R., J. Huang, P. Maness, A. Mohagheghi, S. Czernik and E. Chornet. 2007. Hydrogen production from the fermentation of corn stover biomass pretreated with a steam-explosion process. *Int.J.Hydrogen Energy* 32(8): 932-939.
- Demirbas, A. 2001. Energy balance, energy sources, energy policy, future developments and energy investments in Turkey. *Energy Conversion and Management* 42(10): 1239.
- Deng, Y. and Y. Wang. 2009. The kinetics of cellulose dissolution in sodium hydroxide solution at low temperatures. *Biotechnology and Bioengineering* 102(5): 1398.
- Devara, P. and D. Chate. 2009. Acidity of raindrop by uptake of gases and aerosol pollutants. *Atmospheric Environment* 43(8): 1571.
- Dhepe, P. L., M. Ohashi, S. Inagaki, M. Ichikawa and A. Fukuoka. 2005. Hydrolysis of sugars catalyzed by water-tolerant sulfonated mesoporous silicas. *Catalysis Letters* 102(3-4): 163.
- Effendi, A., H. Gerhauser and A. Bridgwater. 2008. Production of renewable phenolic resins by thermochemical conversion of biomass: A review. *Renewable Sustainable Energy Reviews* 12(8): 2092.

- Fan, J. and Y. Gao. 2006. Nanoparticle-supported catalysts and catalytic reactions - a mini-review. *J.Exp.Nanosci.* 1(1-4): 457-475.
- Fukuoka, A. and P. L. Dhepe. 2006. Catalytic conversion of cellulose into sugar alcohols. *Angewandte Chemie-International Edition* 45(31): 5161-5163.
- Gill, C. S., B. A. Price and C. W. Jones. 2007. Sulfonic acid-functionalized silica-coated magnetic nanoparticle catalysts. *Journal of .Catalysis.* 251(1): 145-152.
- Guler, M. O. and S. I. Stupp. 2007. A self-assembled nanofiber catalyst for ester hydrolysis. *Journal of the American Chemical Society* 129(40): 12082.
- Hall, D. O. and P. A. Moss. 1983. Biomass for energy in developing countries. *GeoJournal.* 7(1): 5-5-14.
- Harmer, M. A., W. E. Farneth and Q. Sun. 1998. Towards the sulfuric acid of solids. *Advanced Materials* 10(15): 1255.
- Harmer, M. A., W. E. Farneth and Q. Sun. 1996. High surface area nafion resin/silica nanocomposites: A new class of solid acid catalyst. *Journal of the American Chemical Society* 118(33): 7708.
- Harmer, M. A., Q. Sun, M. J. Michalczyk and Z. Y. Yang. 1997. Unique silane modified perfluoroalkyl-sulfonic acids as versatile reagents for new solid acid catalysts. *Chemical Communications*(18): 1803.
- Harmer, M. A., Q. Sun, A. J. Vega, W. E. Farneth, A. Heidekum and W. F. Hoelderich. 2000. Nafion resin-silica nanocomposite solid acid catalysts. Microstructure-processing-property correlations. *Green Chemistry* 2(1): 7.
- Harmer, M. A., C. Junk, V. Rostovtsev, L. G. Carcani, J. Vickery and Z. Schnepf. 2007. Synthesis and applications of superacids. 1,1,2,2-tetrafluoroethanesulfonic acid, supported on silica. *Green Chemistry* 9(1): 30.

- Hart, M., G. Fuller, D. R. Brown, J. A. Dale and S. Plant. 2002. Sulfonated poly(styrene-co-divinylbenzene) ion-exchange resins: acidities and catalytic activities in aqueous reactions. *Journal of Molecular Catalysis. A, Chemical* 182(1): 439.
- Hashimoto, A., J. Fenske, M. Penner and A. Esteghlalian. 1997. Modeling and optimization of the dilute-sulfuric-acid pretreatment of corn stover, poplar and switchgrass. *Bioresource Technology* 59(2-3): 129.
- Herrera, A., S. J. Tellez-Luis, J. A. Ramirez and M. Vazquez. 2003. Production of xylose from sorghum straw using hydrochloric acid. *Journal of Cereal Science* 37(3): 267.
- Herrera, A., S. J. Tellez-Luis, J. J. Gonzalez-Cabriales, J. A. Ramirez and M. Vazquez. 2004. Effect of the hydrochloric acid concentration on the hydrolysis of sorghum straw at atmospheric pressure. *Journal of Food Engineering* 63(1): 103.
- Hyeon, T. 2003. Chemical synthesis of magnetic nanoparticles. *Chem. Commun. (Cambridge, U.K.)*(8): 927-934.
- Iborra, S., A. Corma and G. Huber. 2006. Synthesis of transportation fuels from biomass: Chemistry, catalysts, and engineering. *Chemical Reviews* 106(9): 4044.
- International Trade Commission and Jim Jordan and Associates. 2009. U.S. fuel ethanol industry plants and production capacity. Available at: <http://www.ethanolrfa.org/industry/statistics/>. Accessed 04/27 2009.
- Jacobsen, S. E. and C. E. Wyman. 2002. Xylose monomer and oligomer yields for uncatalyzed hydrolysis of sugarcane bagasse hemicellulose at varying solids concentration. *Industrial Engineering Chemistry Research* 41(6): 1454.
- Janssen, L., H. J. Heeres and B. Girisuta. 2007. Kinetic study on the acid-catalyzed hydrolysis of cellulose to levulinic acid. *Industrial Engineering Chemistry Research* 46(6): 1696.

- Kim, C.; Y. Ryu and C. Park. 2001. Kinetics and rate of enzymatic hydrolysis of cellulose in supercritical carbon dioxide. *Korean Journal of Chemical Engineering* 18(4):475.
- Kim, T.H.; Y.H. Im and Y.B. Hahn. 2003. Plasma enhanced chemical vapor deposition of low dielectric constant SiCFO thin films. *Chemical Physics Letters* 368(1-2): 36.
- Kim, T. H., Y. H. Im and Y. B. Hahn. 2005. Functionalized gold nanoparticles mimic catalytic activity of a polysiloxane-synthesizing enzyme. *Advanced Materials* 17(10): 1234.
- Kim, N., M. Jiang, J. Kang, H. Chang and H. La. 2009. Simultaneous saccharification and fermentation of lignocellulosic residues pretreated with phosphoric acid-acetone for bioethanol production. *Bioresource Technology* 100(13): 3245.
- Kim, T. H. and Y. Y. Lee. 2005. Pretreatment and fractionation of corn stover by ammonia recycle percolation process. *Bioresource Technology*. 96(18): 2007-2013.
- Li, X. M., V. Paraschiv, J. Huskens and et al. 2003. Sulfonic acid-functionalized gold nanoparticles: A colloid-bound catalyst for soft lithographic application on self-assembled monolayers. *Journal of the American Chemical Society* 125(14): 4279.
- Li, Y., K. Klabunde and O. Koper. 1993. Destructive adsorption of chlorinated hydrocarbons on ultrafine (nanoscale) particles of calcium-oxide. *Chemistry of Materials* 5(4): 500.
- Lien, H. L. and W. X. Zhang. 2007. Removal of methyl tert-butyl ether (MTBE) with Nafion. *Journal of Hazardous Materials* 144(1-2): 194.
- Lin, H., J. Wen, N. C, X. YU, G. Tsao and Y. Zheng. 1995. Supercritical Carbon-Dioxide Explosion as a Supercritical Carbon-Dioxide Explosion as a Pretreatment for Cellulose Hydrolysis. *Biotechnology Letters* 17(8): 845.

- Liu, C.G. and Wyman, C.E. 2005. Partial flow of compressed-hot water through corn stover to enhance hemicellulose sugar recovery and enzymatic digestibility of cellulose. *Bioresource Technology* 96(18): 1978.
- Liu, C. and C. E. Wyman. 2004. Effect of the flow rate of a very dilute sulfuric acid on xylan, lignin, and total mass removal from corn stover. *Industrial & Engineering Chemistry Research*. 43(11): 2781-2788.
- Lopezasantin, J., C. Sola and G. Caminal. 1985. Kinetic modeling of the enzymatic-hydrolysis of pretreated cellulose. *Biotechnology and Bioengineering* 27(9): 1282.
- Lou, X., H. W. Wu and Y. Yu. 2008. Some recent advances in hydrolysis of biomass in hot-compressed, water and its comparisons with other hydrolysis methods. *Energy fuels* 22(1): 46.
- McMillan, J. 1994. Pretreatment of Lignocellulosic Biomass. *American Chemical Society Symposium Series*. 566:292.
- Margelefsky, E. L., R. K. Zeidan, V. Dufaud and M. E. Davis. 2007. Organized Surface Functional Groups: Cooperative Catalysis via Thiol/Sulfonic Acid Pairing. *Journal of American Chemical .Society*. 129(44): 13691-13697.
- Martinez, A. and A. Corma. 1993. Chemistry, catalysts, and processes for isoparaffin-olefin alkylation - actual situation and future-trends. *Catalysis Reviews: Science and Engineering* 35(4): 483.
- McCarty, G. S. and P. S. Weiss. 1999. Scanning Probe Studies of Single Nanostructures. *Chem.Rev.(Washington, D.C.)* 99(7): 1983-1990.
- Melero, J. A., G. D. Stucky, R. van Grieken and G. Morales. 2002. Direct syntheses of ordered SBA-15 mesoporous materials containing arenesulfonic acid groups. *Journal of Materials Chemistry* 12(6): 1664.

- Moldes, A. B., J. L. Alonso and J. C. Parajo. 2001. Strategies to improve the bioconversion of processed wood into lactic acid by simultaneous saccharification and fermentation. *Journal of Chemical Technology and Biotechnology* 76(3): 279.
- Mosier, N., C. Wyman, B. Dale, R. Elander, Y. Y. Lee, M. Holtzaple and M. Ladisch. 2005. Features of promising technologies for pretreatment of lignocellulosic biomass. *Bioresource Technology*. 96(6): 673-686.
- Mosier, N. S., A. Sarikaya and M. R. Ladisch. 2000. Structure/function studies for the construction of a cellulolytic enzyme mimetic. In BIOT-004.
- Muller, S., J. Muhlemann, A. Wiedmer, R. Schwarzenbach and M. Berg. 2000. Concentrations and mass fluxes of chloroacetic acids and trifluoroacetic acid in rain and natural waters in Switzerland. *Environmental Science Technology* 34(13): 2675.
- Nathan S. Mosier, Christine M. Ladisch, Michael R. Ladisch. 2002. Characterization of acid catalytic domains for cellulose hydrolysis and glucose degradation. *Biotechnology and Bioengineering*. 79(6):610
- Nilsson, A., M. F. Gorwa-Grauslund, B. Hahn-Hagerdal and G. Liden. 2005. Cofactor dependence in furan reduction by *Saccharomyces cerevisiae* in fermentation of acid-hydrolyzed lignocellulose. *Applied and Environmental Microbiology* 71(12): 7866.
- Oliva, J. M., M. J. Negro and F. Saez. 2006. Effects of acetic acid, furfural and catechol combinations on ethanol fermentation of *Kluyveromyces marxianus*. *Process Biochemistry* 41(5): 1223.
- Onda, A., T. Ochi and K. Yanagisawa. 2008. Selective hydrolysis of cellulose into glucose over solid acid catalysts. *Green Chemistry* 10(10): 1033.
- Pang, Y., Y. Liu, X. Li, K. Wang and Y. He. 2008. Physicochemical characterization of rice straw pretreated with sodium hydroxide in the solid state for enhancing biogas production. *Energy Fuels* 22(4): 2775.

Pankhurst, Q. A., J. Connolly, S. K. Jones and J. Dobson. 2003. Applications of magnetic nanoparticles in biomedicine. *Journal of Physics. D, Applied physics* 36(13): R167.

Perlack, R. D., L. L. Wright, A. F. Turhollow, R. L. Graham, B. J. Stokes and D. C. Erback. 2005. Biomass as feedstock for bioenergy and bioproducts industry: Technical feasibility of a billion-ton annual supply. sponsored by USDOE and USDA. Available at: [http://feedstockreview.ornl.gov/pdf/billion\\_ton\\_vision.pdf](http://feedstockreview.ornl.gov/pdf/billion_ton_vision.pdf).

Petenate, A., M. Meireles and S. Moreschi. 2004. Hydrolysis of ginger bagasse starch in subcritical water and carbon dioxide. *Journal of Agricultural and Food Chemistry* 52(6): 1753.

Phan, N. T. S. and C. W. Jones. 2006. Highly accessible catalytic sites on recyclable organosilane-functionalized magnetic nanoparticles: An alternative to functionalized porous silica catalysts. *Journal of Molecular Catalysis. A, Chemical* 253(1-2): 123.

Rac, B., A. Molnar, P. Forgo, M. Mohai and I. Bertoti. 2006. A comparative study of solid sulfonic acid catalysts based on various ordered mesoporous silica materials. *Journal of Molecular Catalysis. A, Chemical* 244(1-2): 46.

Rhodes, A. 1994. World crude capacity, conversion capability inch upward. *Oil Gas Journal* 92(51): 45.

Rogers, B., J. Adamas and S. Pennathur. 2008. *Nanotechnology, Understanding Small Systems*. Boca Raton, FL: CRC Press.

Rondinone, A. J., A. C. S. Samia and Z. J. Zhang. 1999. Superparamagnetic relaxation and magnetic anisotropy energy distribution in CoFe<sub>2</sub>O<sub>4</sub> spinel ferrite nanocrystallites. *Journal of Physical Chemistry B* 103(33): 6876.

Rothkopf, G. 2007. A Blueprint for Green Energy in the Americas. Available at: <http://idbdocs.iadb.org/wsdocs/getdocument.aspx?docnum=945774>. Retrieved on 2009-09-04.

Roukes, M. 2001. Plenty of room indeed - There is plenty of room for practical innovation at the nanoscale. But first, scientists have to understand the unique physics that governs matter there. *Scientific American* 285(3): 48.

Ruth, M. F., C. E. Wyman and M. E. Himmel. 1999. Cellulase for commodity products from cellulosic biomass. *Current Opinion in Biotechnology* 10(4): 358.

Ryu, Y., C. Kim and C. Park. 2001. Kinetics and rate of enzymatic hydrolysis of cellulose in supercritical carbon dioxide. *Korean Journal of Chemical Engineering* 18(4): 475.

Saeman, J. F. 1945. Kinetics of wood saccharification. Hydrolysis of cellulose and decomposition of sugars in dilute acid at high temperature. *Industrial Engineering Chemistry* 3743-43-52.

Saha, B. C. and J. Woodward, eds. 1997. *Fuels and Chemicals from Biomass*. Washington, D.C.: American Chemical Society.

Saha, B. C. 2003. Hemicellulose bioconversion. *J. Ind. Microbiol. Biotechnol.* 30(5): 279-291.

Salvado, J. and N. El Mansouri. 2006. Structural characterization of technical lignins for the production of adhesives: Application to lignosulfonate, kraft, soda-anthraquinone, organosolv and ethanol process lignins. *Industrial Crops and Products* 24(1): 8.

Selig, M., N. Weiss and Y. Ji. 2008. Enzymatic saccharification of lignocellulosic biomass. NREL/TP-510-42629.

Scaranto, J., A. P. Charmet and S. Giorgianni. 2008. IR spectroscopy and quantum-mechanical studies of the adsorption of CH<sub>2</sub>CClF on TiO<sub>2</sub>. *Journal of Physical Chemistry. C* 112(25): 9443.

Siril, P. F., A. D. Davison, J. K. Randhawa and D. R. Brown. 2007. Acid strengths and catalytic activities of sulfonic acid on polymeric and silica supports. *Journal of Molecular Catalysis. A, Chemical* 267(1-2): 72.

Sluiter, A., B. Hames, R. Ruiz, C. Scarlata, J. Sluiter and D. Templeton. 2008. Determination of sugars, byproducts, and degradation products in liquid fraction process samples. NREL/TP-510-42623.

Sousa, L., S. Chundawat, D. Marshall, L. Sharma, C. Chambliss and V. Balan. 2009. Enzymatic Digestibility and Pretreatment Degradation Products of AFEX-Treated Hardwoods (*Populus nigra*). *Biotechnology Progress* 25(2): 365.

Sperling, D. and D. Gordon. 2009. Brazilian Cane Ethanol: A Policy Model. In *Two billion cars: driving toward sustainability*, 95-96. ed. Anonymous, New York: Oxford University Press.

Suganuma, S., K. Nakajima, M. Kitano, D. Yamaguchi, H. Kato, S. Hayashi and M. Hara. 2008. Hydrolysis of cellulose by amorphous carbon bearing SO<sub>3</sub>H, COOH, and OH groups. *Journal of the American Chemical Society* 130(38): 12787.

Sun, Y., J. Zhuang, L. Lin and P. Ouyang. 2009. Clean conversion of cellulose into fermentable glucose. *Biotechnology Advances* 27(5): 625.

Sun, L., I. Negulescu, M. Moore, B. Collier and Y. Chen. 2005. Evaluating efficiency of alkaline treatment for waste bagasse. *Journal of Macromolecular Science. Physics* 44(3): 397.

Teymouri, F., T. Gilbert, B. Dale and H. Alizadeh. 2005. Pretreatment of switchgrass by ammonia fiber explosion (AFEX). *Applied Biochemistry and Biotechnology* 121:1133.

Teymouri, F., L. Laureano-Perez, H. Alizadeh and B. Dale. 2004a. Ammonia Fiber Explosion Treatment of Corn Stover. *Applied Biochemistry and Biotechnology* 115(4): 951-951-963.

Teymouri, F., L. Laureano-Perez, H. Alizadeh and B. E. Dale. 2004b. Ammonia fiber explosion treatment of corn stover. *Appl.Biochem.Biotechnol.* 113-116951-963.

U.S. Department of Energy. 2006. Concentrated Acid Hydrolysis.

Van Dyne, D., Y. Choi, N. Blase and M. Kaylen. 2000. Economic feasibility of producing ethanol from lignocellulosic feedstocks. *Bioresource Technology* 72(1): 19.

Van Hooijdonk, G., A. Faaij and C. Hamelinck. 2005. Ethanol from lignocellulosic biomass: techno-economic performance in short-, middle- and long-term. *Biomass Bioenergy* 28(4): 384.

Van Rhijn, W. M., D. E. De Vos, B. F. Sels, W. D. Bossaert and P. A. Jacobs. 1998. Sulfonic acid functionalized ordered mesoporous materials as catalysts for condensation and esterification reactions. *Chem.Commun.(Cambridge)*(3): 317-318.

Van Siclen, C. and H. Farrell. 2007. Binding energy, vapor pressure, and melting point of semiconductor nanoparticles. *Journal of Vacuum Science Technology* 25(4): 1441.

Varga, E., K. Reczey and G. Zacchi. 2004. Optimization of Steam Pretreatment of Corn Stover to Enhance Enzymatic Digestibility. *Applied Biochemistry and Biotechnology* 114(4): 509-509-523.

Viola, E., F. Nanna, E. Larocca, M. Cardinale, D. Barisano and F. Zimbardi. 2007. Acid impregnation and steam explosion of corn stover in batch processes. *Industrial Crops and Products* 26(2): 195.

Vriezema, D. M., M. C. Aragonés, J. A. A. W. Elemans, J. J. L. M. Cornelissen, A. E. Rowan and R. J. M. Nolte. 2005. Self-assembled nanoreactors. *Chemical Reviews* 105(4): 1445.

Wyman, C. E., B. E. Dale, R. T. Elander, M. Holtzapple, M. R. Ladisch and Y. Y. Lee. 2005. Coordinated development of leading biomass pretreatment technologies. *Bioresour.Technol.* 96(18): 1959-1966.

Yang, B. and C. E. Wyman. 2004. Effect of xylan and lignin removal by batch and flowthrough pretreatment on the enzymatic digestibility of corn stover cellulose. *Biotechnol.Bioeng.* 86(1): 88-95.

Yang, B.Y. and R. Montgomery. 1996. Alkaline degradation of glucose: Effect of initial concentration of reactants. *Carbohydrate Research.* 280(1):27-45.

Yoon, T., W. Lee, Y. Oh and J. Lee. 2003. Magnetic nanoparticles as a catalyst vehicle for simple and easy recycling. *New J.Chem.* 27(2): 227-229.

Zhang, M., B. L. Cushing and C. J. O'Connor. 2008. Synthesis and characterization of monodisperse ultra-thin silica-coated magnetic nanoparticles. *Nanotechnology* 19(8): 085601.

Zhao, X. S., G. Q. Lu and X. Hu. 2000. Characterization of the structural and surface properties of chemically modified MCM-41 material. *Microporous and Mesoporous Materials* 4137-37-47.

Zhao, Y., W. Lu and H. Wang. 2009. Supercritical hydrolysis of cellulose for oligosaccharide production in combined technology. *Chemical Engineering Journal.* 150(2-3):411.

Zheng, Y., C. Duanmu and Y. Gao. 2006. A Magnetic Biomimetic Nanocatalyst for Cleaving Phosphoester and Carboxylic Ester Bonds under Mild Conditions. *Org.Lett.* 8(15): 3215-3217.